A CONTRIBUTION TO THE EXPERIMENTAL CHARACTERIZATION OF IMPEDANCE STEPS IN MICROSTRIP

by

Kamal K Masand

A thesis submitted to the School of Graduate Studies,
University of Ottawa, in partial fulfilment
of the requirements for the degree of
Master of Applied Science.

Department of Electrical Engineering
Faculty of Science and Engineering
University of Ottawa
Ottawa, Canada
September, 1976

ACKNOWLEDGEMENTS

The author feels happy to acknowledge the invaluable suggestions and guidance during the preparation of the thesis by his supervisor Dr. W.J.R.Hoefer. The conceptual and sound knowledge of Dr. Hoefer has certainly been encouraging and beneficial. The fruitful discussions with Prof. W.Steenaart have been indispensable.

The financial assistance received from the Department of Electrical Engineering, University of Ottawa, during the course of this thesis is also earnestly and gratefully appreciated. Finally, the author is thankful to Dr. D.S.James for supplying the ring-resonator.

ABSTRACT

A sudden step change in the width of a microstrip has been characterized thorugh measurement. A resonant ring method is shown to yield high quality measurements. Inductive and capacitive components of the equivalent circuit of the step discontinuity have been measured for several step ratios. The results agree well with theoretical values available in the literature.

CONTENTS

LIST OF TABLES

LIST OF FIGURES

Contd

LIST OF FIGURES - Contd

CHAPTER 1

INTRODUCTION

1.1 SYNOPSIS

Miniaturization of microwave circuits into microwave integrated circuits is impossible without microstrip transmission lines and microstrip circuit elements. A microstrip is a transmission line which consists of a single thin conducting strip and a ground plane, on opposite faces of a sheet of dielectric material as shown in figure 1.1. Its simple and economic fabrication by thin or thick film printed circuit techniques is the main reason for which the use of microstrip lines has dominated other types of transmission lines like strip line or coaxial line.

A microstrip discontinuity may be defined as the geometric area in which the properties such as characteristic impedance or phase velocity change. Common examples are right angle bends, T-junctions or sudden changes in the width of the microstrip. The modeling of microstrip discontinuities in terms of lumped equivalent circuits has recently been a subject of intense interest in the field of microwaves.

The so called impedance step, an abrupt change in the width of the microstrip transmission line has been investigated by many authors [1-4,6] . Most of the work is theoretical however, and the experimental work is insufficient to date to verify completely the theoretical characterization of this discontinuity. Therefore, it is thought that an experimental contribution to the characterization of impedance steps is quite desirable.

In this thesis, the equivalent circuit of impedance steps in microstrip will be determined experimentally using resonant ring method [8] , and the results will be compared with available theoretical values.

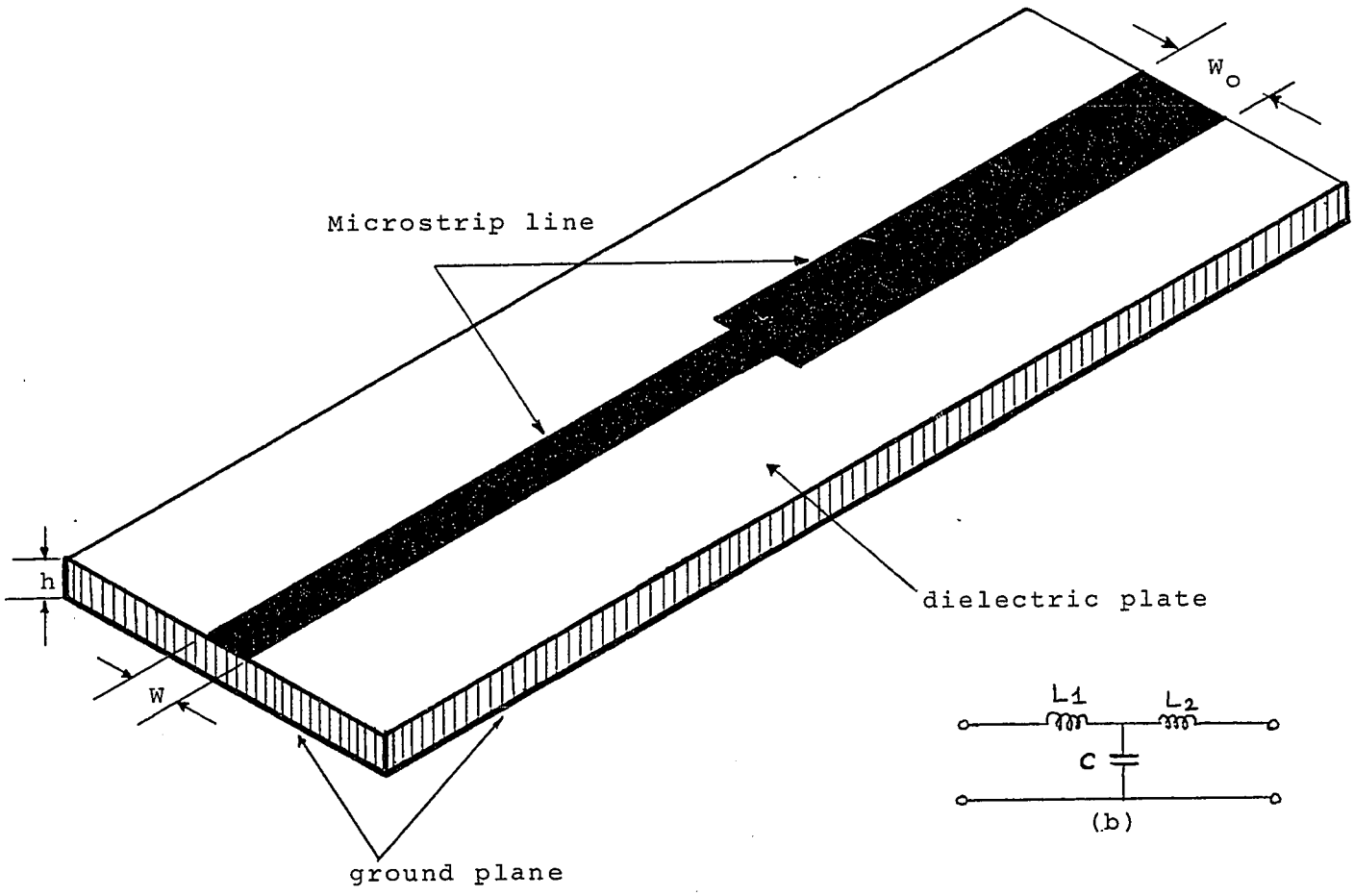

Figure 1.1: Typical microstrip line with a discontinuity, the sudden change in the width of a microstrip line. (b) shows the equivalent circuit for the step discontinuity.

1.2 LITERATURE SURVEY OF THEORETICAL AND EXPERIMENTAL METHODS TO DETERMINE THE PARAMETERS OF AN ABRUPT CHANGE IN THE WIDTH OF A MICROSTRIP

In April 1972, Wolff et al [1] , published some results on theoretically calculated transmission coefficients for sudden step changes in width of a microstrip line. It was shown that the scattering matrix for the discontinuity depends strongly on the frequency if the substrate material is of small relative permittivity. The frequency dependance was small for alumina substrate which has a higher relative permittivity. An approximate wave guide model of the microstrip line and well tested methods for calculating discontinuities and jucntions in waveguides were used. These methods use orthogonal series expansion functions of the fields in the waveguide. The limitation of this method is that a complete set of field solutions must be known for the structures considered before applying series expansion methods. A further condition is that the solutions should be orthogonal. As is well known, no complete set of solutions for the field problem of microstrip line has yet been published. However, Wolff et al took the waveguide model given by Wheeler [7] for the lowest order mode, which to a first approximation is a TEM mode and then assumed that it would describe the higher modes in the microstrip as well.

In August 1972, Farrar and Adams [2] , applied matrix methods for solution to three dimensional microstrip problems with emphasis upon the discontinuities in microstrips. Point matching (impulsive weights) was used with pulse expansion functions in order to find the capacitance associated with the impedance step in the microstrip line. They have ignored the inductive effect associated with the impedance step, stating that the method is suitable to microstrip discontinuities in which capacitive effects predominate. The advantage of

this method resides in the ease with which the matrix equations can be solved on a digital computer. Also geometric progression has been used gor non uniform subsectioning the microstrip. This measure saves computing time without compromising accuracy. The disadvantage of this method resides in the assumption of occurence of the quasi-static TEM mode propagation on the microstrip line and the long computing times, of the order of 7 to 18 minutes, also taking symmetry of the discontinuity into consideration. Thus, this method is not an economic one for determining the parameters of a microstrip discontinuity. One reason for large computing times is that as W/H (the aspect ratio) decreases, the fringing effects become more important and more terms of the source function which is represented by an infinite series are required. This series converges very slowly. Also because of this the error in the results is always of the order of few percent.

In August 1973, Horton [3], reported an equivalent representation of an abrupt impedance step in microstrip line. His calculations are based on the assumption that static current paths occur in such a structure, which consequently impose the limitation of quasi TEM propagation on the microstrip line. Equivalent lengths of transmission lines ascribable to the impedance step were given and this information in calculating the capacitance associated with the step was used. Thus, Horton's results correct the results obtained by Farrar and Adams by taking into account the associated inductance.

In February 1975, Groll and Weidmann [4], published the measurement results obtained through a measurement technique. A circular resonant ring was used and the change in resonance frequency ascribable to the impedance step was measured. However, in order to determine the equivalent circuit they designed the microstrip resonator in such a way that at resonance, nodes and antinodes of

RF currents were located at the discontinuity. In case of current node at the step parallel elements were effective only. At antinodes, series components could be measured only. The localization of nodes and antinodes was achieved by special coupling which is the limitation of this method since the nodes and antinodes at the discontinuity at all modes of resonance cannot be obtained accurately. Thus, the method introduces an additional source of error due to the uncertainty in the position of nodes and antinodes.

In December 1975, Akhtarzad and Johns [5], reported the dispersion characteristics of this discontinuity. They applied Transmission Line Matrix (TLM) method which is computer based. This method simulates Maxwell's Equations on a three dimensional mesh of transmission lines and solves these equations in time domain subject to the appropriate boundary conditions. Any of the six electromagnetic components can be excited by introducing impulses at various points in the network model. The output consists of stream of impulses with amplitude corresponding to the output impulse function for the particular field component under consideration. The Fourier transform of this method is taken to yield the response to an excitation varying sinusoidally with time. The advantage of this method resides in the general versatility of the computing method; does not assume quasi TEM mode of propagation; and contains information about higher modes since it operates in the time domain. However, the computing times are of the order of 2 to 10 minutes on an ICL - 1906A computer.

In March 1976, Gopinath, Thomson and Stephenson [6], applied a variational technique to find the inductive component of the equivalent circuit of the impedance step. For experimental measurements they used straight through resonators with end effect quite nearly calibrated as discussed by Easter [9]. The theoretical and experimental values for inductance were in good agreement. The reason

for error was that their trial functions did not describe adequately the current distribution around the corners. However, Gopinath et al have not evaluated the capacitive component of the equivalent circuit as it has been evaluated by other authors. However, the method is suitable for evaluating only the inductive components of the equivalent circuits of microstrip discontinuities.

1.3 Thesis Approach

The objective of this thesis is to characterize the sudden step in the width of a microstrip through measurement. The measurement was performed in the following steps:

(1) The resonant ring with a discontinuity (figure 1.2) was fabricated. This fabrication was done at the Communications Research Centre, Ottawa.

(2) The resonant frequencies at fundamental and higher modes for even and odd excitation of the discontinuity were measured as described in Chapter 3.

(3) The step size was reduced and resonance frequencies were measured for even and odd excitation to obtain results for different w/w_o.

(4) The step was removed i.e. $w = w_o$ and again resonance frequencies were measured. This was done to find the dispersion characteristics of the empty ring itself. Normally, this would have been done first but it was easier to reduce the discontinuity step by step than to add to it. Throughout the measurement care was taken to stabilize the temperature of the ring as described in Chapter 3.

(5) The admittance of the impedance step was calculated from the change of resonant

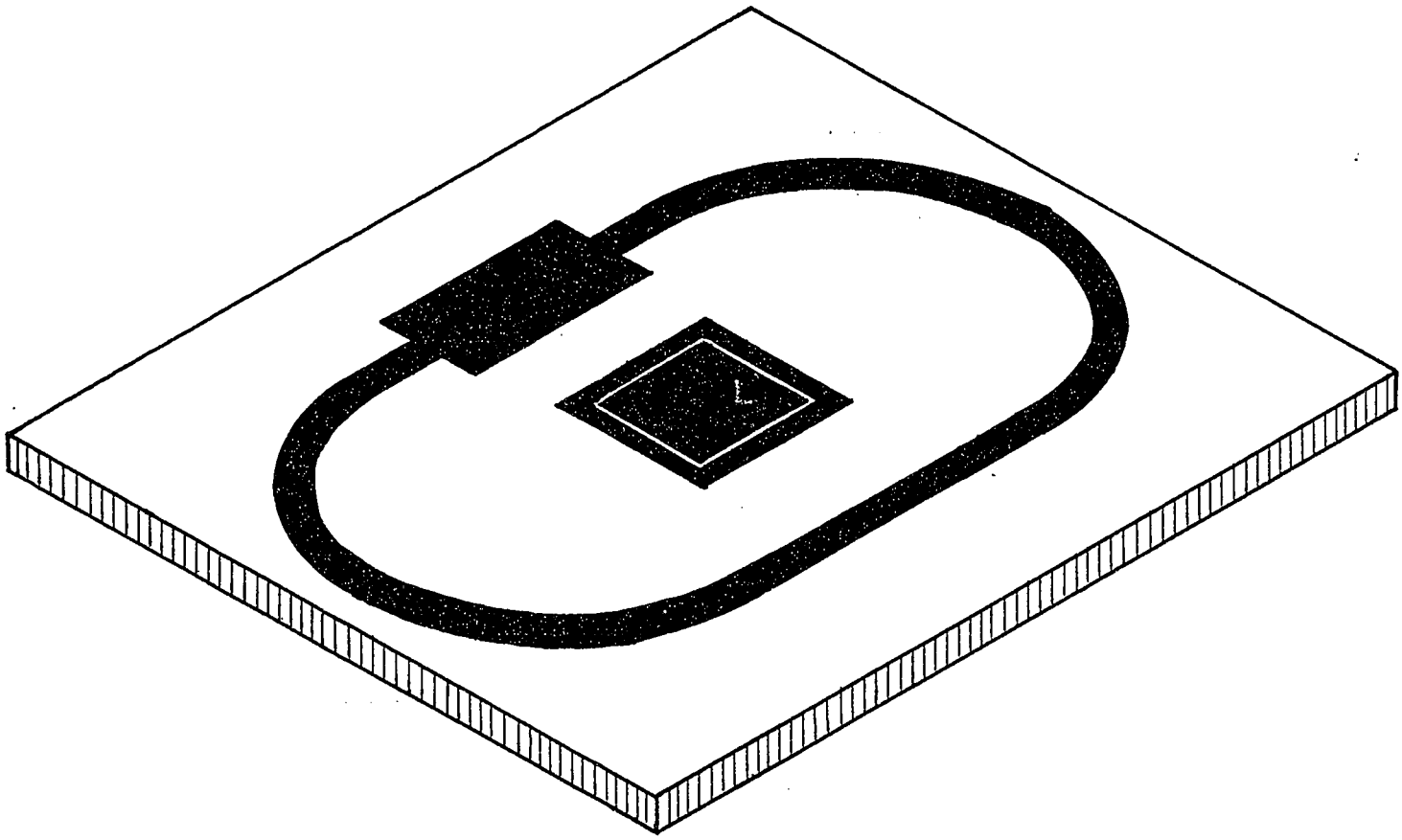

Figure 1.2: Isometric view of the ring resonator which was used for measurements. Detailed dimensions are given in Figure 2.1.

frequencies as described in Chapter 2. Error analysis was done for every measured value as described in Chapter 4.

(6) Finally, the results were compared with the results obtained by other authors.

1.4 Reasons for using the Resonant Ring Method

(1) As it has been observed in the literature survey, no theoretical technique has given the exact analysis of this discontinuity. Thus, by including dispersion, and hybrid mode of propagation in microstrip, need arises to characterize it experimentally.

(2) The very small effects to be measured complicate the evaluation of the discontinuity. Because of the short electrical length of the discontiniuty some common methods like s-parameter measurement will not be sufficiently precise. Further, the transitions and the package will cause error of the same magnitude as the discontinuity itself.

(3) The only assumption made in the resonant ring method is that the strip width is much smaller than the radius of curvature of the ring; in order to avoid field distortion due to curvature and minimize coupling between different parts of the ring.

(4) The resonant ring has advantage over straight through resonators that one must not account for the end effects, described by Easter [9].

(5) The resonant frequencies can be measured with great accuracy using digital frequency counters.

CHAPTER 2

THEORY

2.1 ANALYSIS OF THE RESONANT RING CONTAINING AN ABRUPT STEP CHANGE IN THE WIDTH OF THE MICROSTRIP

A. Chattopadhyay and W. Hoefer [8] have applied a measurement technique using a resonant ring for evaluating any reciprocal microstrip discontinuity. A similar approach is chosen here.

In Fig. 2.1 a sudden change in the width of a microstrip is shown. Uniform microstrip lines exist before and after the plane of discontinuity. The question is what happens at the plane or near the plane of discontinuity. As is apparent the electric field will be distorted in the region near the discontinuity, but after some distance it will be homogeneous again.

When either electric or magnetic field components are aligned in the direction of propagation, higher modes are launched. Discontinuities in microstrips, effectively, launch certain higher order modes, and energy will be stored in these modes. However, these higher modes decrease their magnitude exponentially, and will be attenuated accordingly. It is well known from lumped circuit theory that energy storage will occur where capacitance or inductance or both are present. Thus the behaviour of the discontinuity is characterized by an equivalent circuit made up of lumped reactive elements.

The ring will resonate if its electrical length is an integral multiple of the guided wave length. When a discontinuity is introduced into the ring each resonance degenerates into two distinct modes. The splitting is conveniently interpreted in terms of even and odd excitation of the ring. The even case corresponds

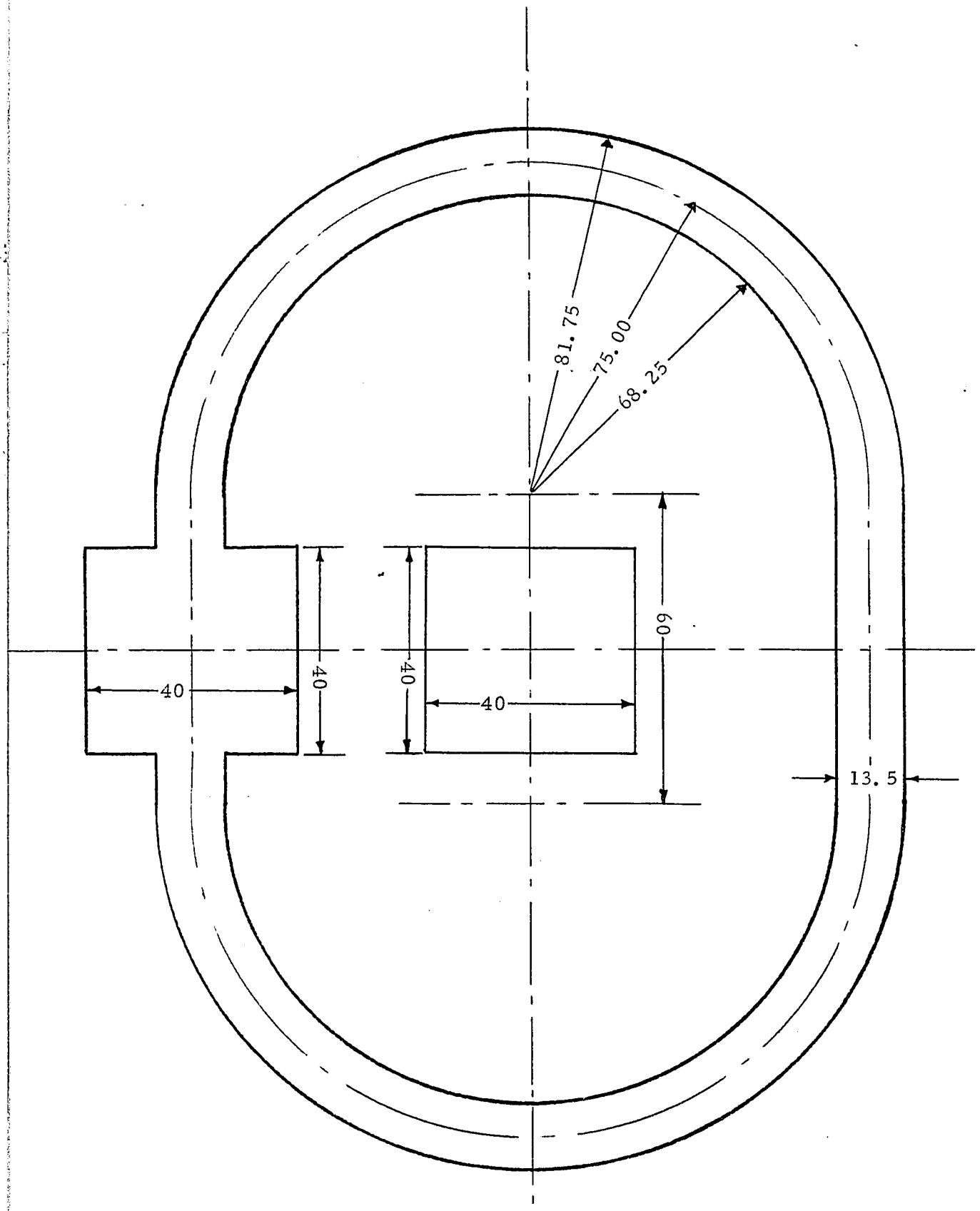

Fig. 2.1: Ring resonator containing the discontinuity ; the step change in the width of a microstrip line. All measurements are in millimeters . The thickness of the Stycast substrate (εr=10.97) is 5 mm.

to the incidence of two waves of equal magnitude and phase upon the plane of symmetry on the opposite side of the point of excitation, while in the odd case, waves of equal magnitude but opposite phase are incident from both sides. Either mode of resonance can be achieved separately by an appropriate choice of point of excitation along the ring. Thus,

$$l_{ring} + 2\, l_e - l_w = n\, \lambda_{ge} \quad \text{(even case)} \tag{2.1}$$

and

$$l_{ring} + 2\, l_o - l_w = n\, \lambda_{go} \quad \text{(odd case)} \tag{2.2}$$

where

λ_{ge}, λ_{go} = guided wave length in the structure corresponding to even and odd mode resonance respectively.

l_{ring} = physical length of the ring along the mean circumference.

l_w = physical length of the wide microstrip.

n = harmonic number

l_e, l_o = equivalent fictitious lengths of transmission lines for even and odd mode respectively.

l_{ring} and l_w are known and guided wave length λ_g can be obtained from measurements; l_e and l_o are determined as:

$$l_e = \frac{1}{2}\left[n\, \lambda_{ge} - l_{ring} + l_w\right] \tag{2.3}$$

$$l_o = \frac{1}{2}\left[n\, \lambda_{go} - l_{ring} + l_w\right] \tag{2.4}$$

Since we measure resonance frequencies rather than wavelengths, it is convenient to express the guided wave length as follows:

$$\lambda_{ge} = \frac{c}{f_{re}\{\varepsilon_{eff}(f_{re})\}^{\frac{1}{2}}} \tag{2.5}$$

$$\lambda_{go} = \frac{c}{f_{ro}\{\varepsilon_{eff}(f_{ro})\}^{\frac{1}{2}}} \tag{2.6}$$

where c = velocity of light.

$\varepsilon_{eff}(f)$ = dispersive effective dielectric constant of the ring.

f_{re}, f_{ro} = even and odd mode resonance frequencies respectively.

Since the step change in the width of the microstrip is a lossless discontinuity, only the resonant frequencies of the perturbed ring are affected and even and odd admittances are purely reactive. These admittances may be thought of as input admittances of fictitious transmission line sections which are open for the even mode and short circuited for the odd mode. Fig. 2.2a shows the microstrip resonator straightened out for convenient presentation. In Fig.2.2b, the step discontinuity and the half section of the wider microstrip are represented by a fictitious transmission line of length l_e. The length l_e is such that the input admittance at plane 1 in Fig. 2.2a and b is the same. Similarly, in Fig. 2.3, the representation of the discontinuity by a fictitious transmission line for the odd case is shown. In Figure 2.4a and b the standing wave pattern on the ring resonating in the fundamental mode is shown.

The input admittance at plane 1 for the even and odd mode respectively is given by:

$$Y_{ie} = j\, Y_{01} \tan [\beta l_e] \quad \text{(even mode)} \tag{2.7}$$

$$Y_{io} = -j\, Y_{01} \cot [\beta l_o] \quad \text{(odd mode)} \tag{2.8}$$

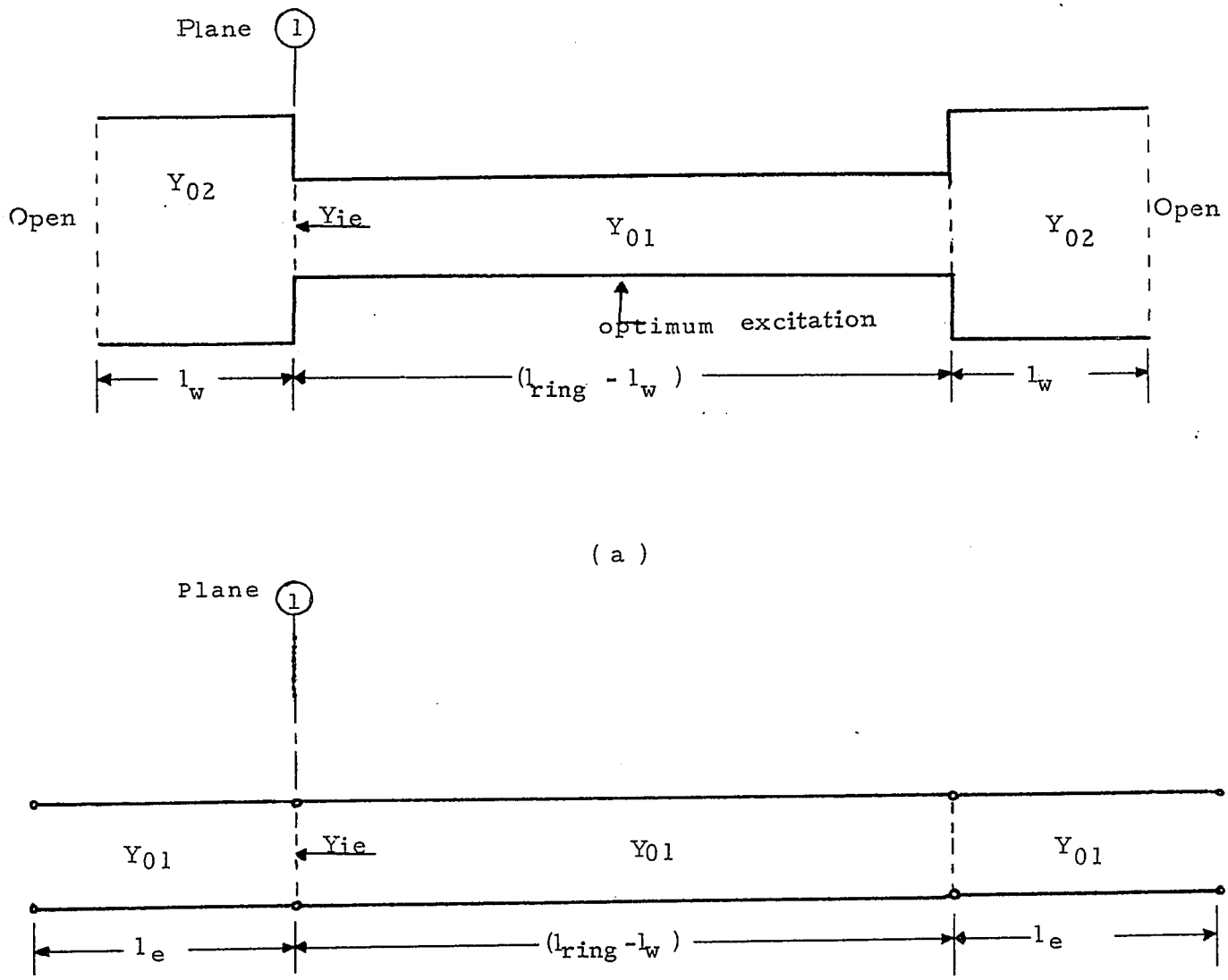

Fig. 2.2: (a) Representation of microstrip resonator for even excitation. The resonator is straightened out for convenient representation. (b) Representation of the discontinuity by a fictitious transmission line of length l_e

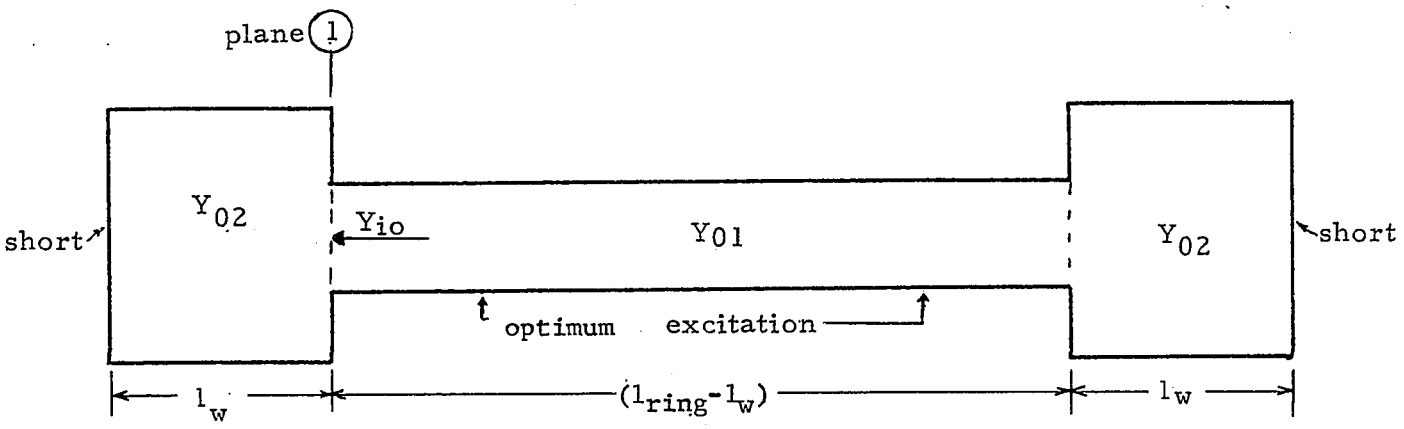

(a)

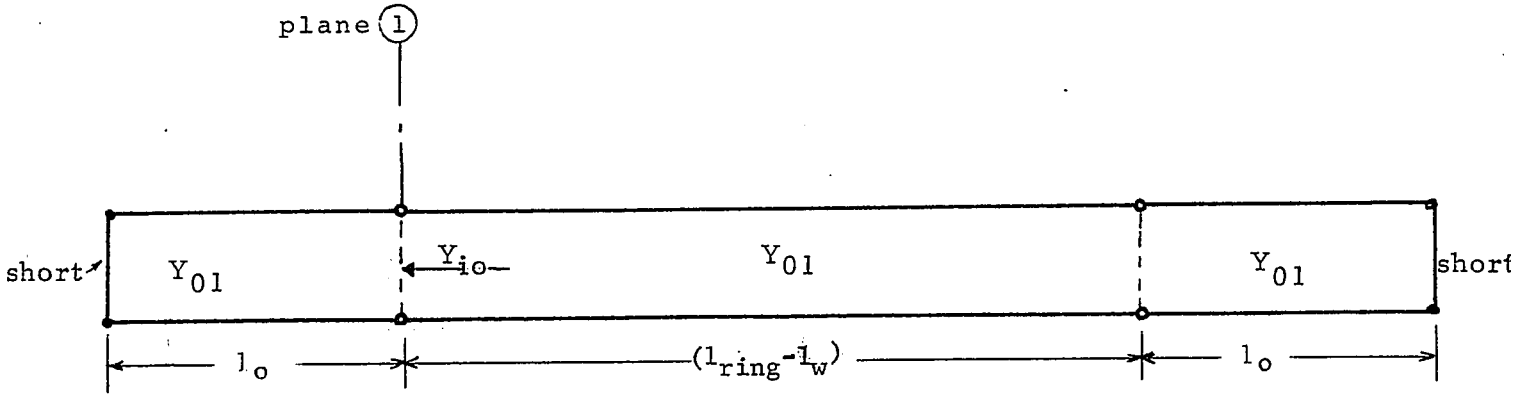

(b)

Fig. 2.3: (a) Representation of the microstrip resonator for odd excitation. (b) The step discontinuity and wide microstrip have been represented by an equivalent fictitious transmission line of length l_o.

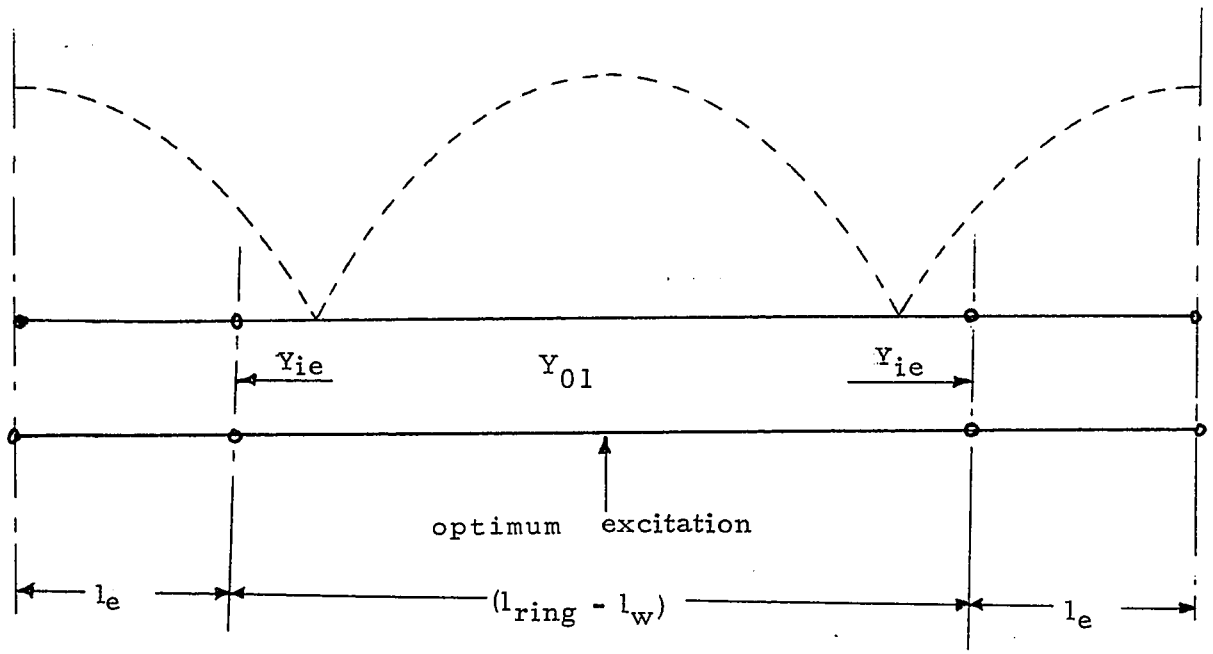

(a)

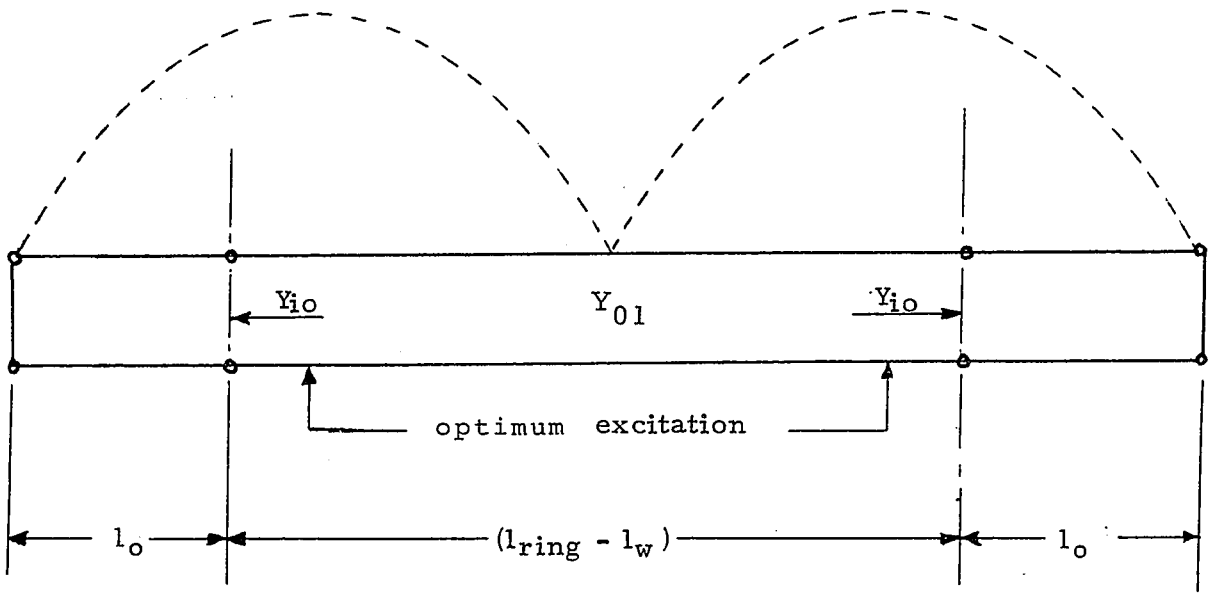

(b)

Fig. 2.4: Standing wave pattern on the ring for resonance in the fundamental mode. (a) for even excitation (b) for odd excitation.

where $\beta = 2\pi/\lambda_g$, is the propagation constant for the quasi TEM mode. Using equations (2.3 and (2.4) we get:

$$Y_{ie} = j\, Y_{01} \tan\left[\tfrac{1}{2}\,\beta\,(n\lambda_{ge} - l_{ring} + l_w)\right] \tag{2.9}$$

$$Y_{io} = jY_{01} \cot\left[\tfrac{1}{2}\,\beta\,(n\lambda_{go} - l_{ring} + l_w)\right] \tag{2.10}$$

substituting the values of λ_{ge} and λ_{go} from equation (2.5) and (2.6) into equations (2.9) and (2.10) respectively and after simplication we get the following expressions:

$$Y_{ie} = -j\, Y_{01}(f_{re}) \tan\left[\frac{\pi\, f_{re} \sqrt{\varepsilon_{eff}(f_{re})}\ \{l_{ring}-l_w\}}{c}\right] \tag{2.11}$$

$$Y_{io} = +j\, Y_{01}(f_{ro}) \cot\left[\frac{\pi\, f_{ro} \sqrt{\varepsilon_{eff}(f_{ro})}\ \{l_{ring}-l_w\}}{c}\right] \tag{2.12}$$

Since the input admittance is the sum of the admittances corresponding to the step discontinuity and half the length of wide microstrip line, we have,

$$Y_{ie} = Y_{step} + Y_{we} \tag{2.13}$$

$$Y_{io} = Y_{step} + Y_{wo} \tag{2.14}$$

where Y_{step} is the admittance associated with the step discontinuity and Y_{we}, Y_{wo} correspond to the input admittances of the wide microstrip for even and odd mode respectively.

Y_{we} and Y_{wo} are defined by the following equations:

$$Y_{we} = j\, Y_{02} \tan\left[\beta\, \frac{l_w}{2}\right] \tag{2.15}$$

$$Y_{wo} = -j\, Y_{02} \cot\left[\beta\, \frac{l_w}{2}\right] \tag{2.16}$$

Introducing equations (2.5) and (2.6) into (2.15) and (2.16):

$$Y_{we} = j\, Y_{02}(f_{re}) \tan\left[\frac{\pi l_w f_{re}\sqrt{\varepsilon_{eff}(f_{re})}}{c}\right] \quad (2.17)$$

$$Y_{wo} = -j\, Y_{02}(f_{ro}) \cot\left[\frac{\pi l_w f_{ro}\sqrt{\varepsilon_{eff}(f_{ro})}}{c}\right] \quad (2.18)$$

Finally, putting the expressions for Y_{ie}, Y_{io} and Y_{we}, Y_{wo} in equations (2.13) and (2.14), we get the expressions for admittance associated with step-discontinuity as given below:

$$Y_{step} = j\left[Y_{02}(f_{re}) \tan\left\{\frac{\pi l_w f_{re}\sqrt{\varepsilon_{eff}(f_{re})}}{c}\right\} - Y_{01}(f_{re}) \tan\left\{\frac{\pi f_{re}\sqrt{\varepsilon_{eff}(f_{re})}(l_{ring}-l_w)}{c}\right\}\right] \quad (2.19)$$

and

$$Y_{step} = j\left[Y_{01}(f_{ro}) \cot\left\{\frac{\pi f_{ro}\sqrt{\varepsilon_{eff}(f_{ro})}\,(l_{ring}-l_w)}{c}\right\} - Y_{02}(f_{ro}) \cot\left\{\frac{\pi f_{ro}\, l_w\sqrt{\varepsilon_{eff}(f_{ro})}}{c}\right\}\right] \quad (2.20)$$

These expressions form the basis of measurement and will be described in the next chapter.

CHAPTER 3

MEASUREMENT TECHNIQUE

As it has been observed in the preceeding chapter that the precise measurement of resonance frequencies is of utmost importance since, the discontinuity admittance values are very sensitive to errors in frequency measurements. The accuracy of the measurement is limited by the sharpness of the response rather than the performance of the available frequency counters for the microwave range. However, errors due to the uncertainty in the resonant frequencies of the ring have been reduced significantly by making several independent measurements of the same resonance, as described later. Before outlining the measurement technique, a brief description of the essential parts of the experimental arrangement will be given.

3.1.1. THE RING RESONATOR

Measurements were performed on a ring which has the shape of a racetrack as shown in figure 1.1 The ring was made as uniform as possible since even small irregularities may produce effects of the same order as the discontinuity to be measured. The discontinuity consisted of a short length of wider strip in a ring of narrow strip (figure 1.1). The static characteristic impedance of the narrow section was about 26 ohms and that of the wide section was about 11 ohms. Stycast substrate with a nominal dielectric constant of 10.97* was used. The thickness of the substrate was 5.0 mm. The mean circumference of the ring was lring = 59.15 centimeters and the length of the wide section was l_w = 4.0 centimeters. Thus, the ring contained two identical impedance steps separated by a distance l_w.

The square of 4 x 4 cm^2 at the center of the ring was used to measure the nominal dielectric constant of the ring.

* The dielectric constant has been measured as described in section 3.3

The resonator was excited by the capacitive launcher which could be moved in order to find the optimum point of excitation along the straight section of the ring on the opposite side of the discontinuity. Coupling was kept as light as the sensitivity of the measuring equipment permitted. Even then, the launcher changed the resonance frequencies slightly. But as long as the measurements on the empty and loaded ring were made at the same coupling strength, the effect of the launcher was eliminated since it affected all the measurements in the same way [14].

3.1.2. TEMPERATURE CHAMBER

The ordinary daily changes in room temperature alter the resonance frequencies of the ring sufficiently to cause unacceptable errors. Therefore, it was necessary to stabilize the temperature of the substrate within $\pm 0.5^{o}C$. A temperature controlled box was designed and the ring was placed in it.

The box as shown in figure 3.1 was lined by a 2.5 inch thick layer of styrofoam on all sides which is a very good temperature isolator. Only the upper lid could be removed to place the microstrip ring inside the box. A cable was introduced into the box through a very small hole in one side of the box and that served as the connection between launcher and peripheral equipment. By pulling or pushing the cable from the outside, the launcher could be placed at the appropriate excitation points along the ring. A temperature probe and an electric light bulb as a heating element were mounted within the box, and they were connected to the temperature control equipment outside the box. During the course of experiments, the temperature inside the box was maintained at $35^{o}C \pm 0.4^{o}C$. To ensure a uniform temperature distribution in the box, it was heated for 5-6 hours and a small fan circulated air continuously at all times. The temperature inside the box was monitored with the help of a thermometer which was introduced through a very small hole in the top lid of the box.

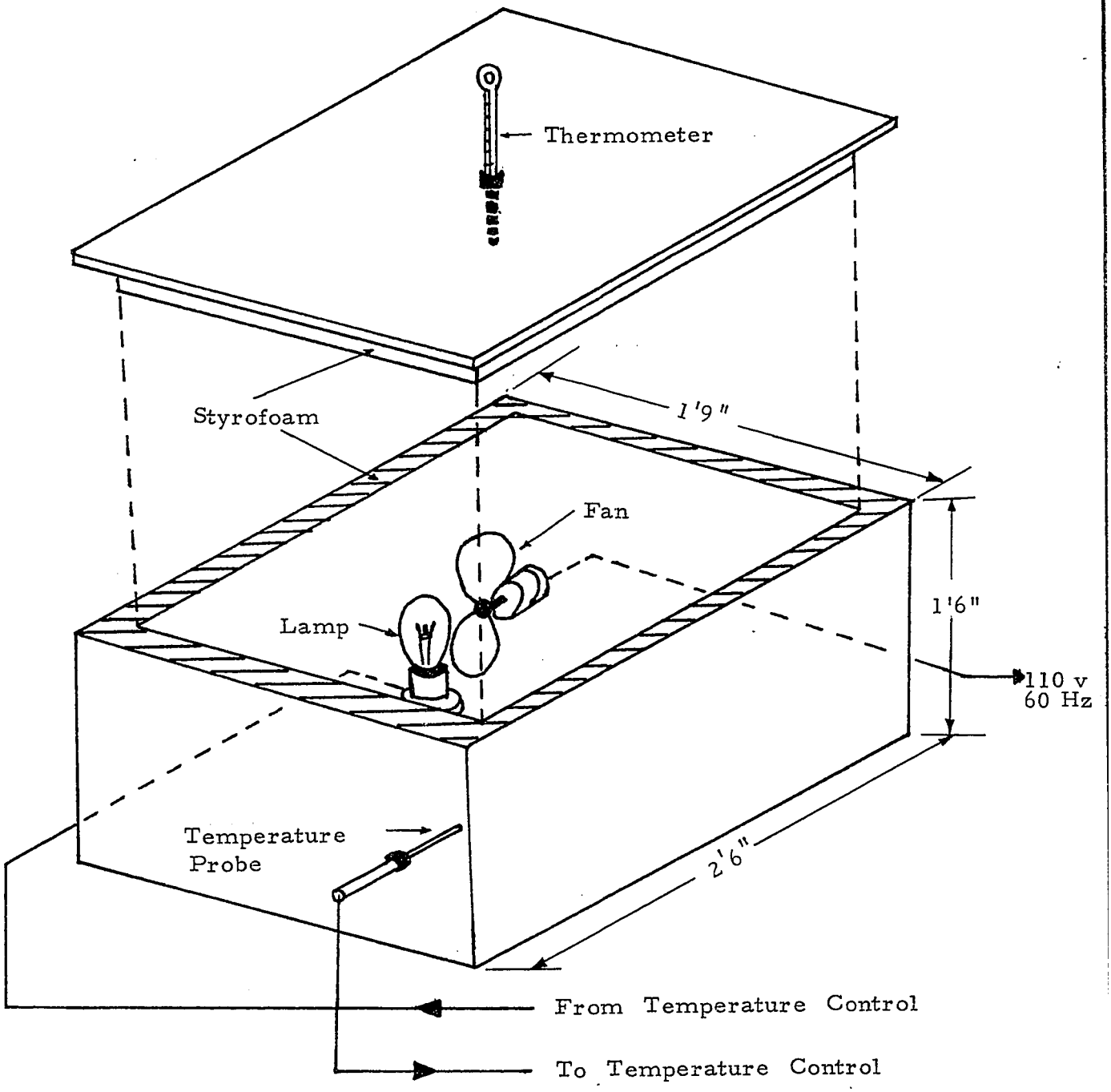

Fig. 3.1: Temperature controlled chamber used for the stabilization of the temperature of the substrate.

3.2 THE MEASUREMENT TECHNIQUE

The schematic diagram for measurement of resonance frequencies is shown in figure 3.2. The reflection characteristics of the resonant ring were measured using a Swept Amplitude Analyzer. A spectrum analyzer was used to compare the resonance frequencies of the ring with the frequency of a precision frequency generator. The output of the frequency generator was displayed on a digital frequency counter. The vertical output of the spectrum analyzer was fed to the Swept Amplitude Analyzer as the Z-axis marker.

Now, we shall describe the procedure followed to determine exactly any particular resonance frequency. To start with, the sweep oscillator was sweeping in Δf mode. By changing the central frequency of the sweep, the response of the ring was centered on the screen of the Swept Amplitude Analyser. Then the sweep was changed to manual and the output frequency of the sweep oscillator was set as close to the peak as possible. Now the local oscillator of the spectrum analyzer was adjusted and tuned such that the local oscillator frequency was in the center of the spectrum analyzer screen. The the scanning mode of the spectrum analyzer was changed to manual. The sweeper was again swept in automatic mode at a very low speed. The vertical output of the spectrum analyzer density modulated the display of the Swept Amplitude Analyzer, producing a dot on the absorption curve very near to its peak. The frequency of the spectrum analyzer was now finally adjusted to place the dot exactly on the peak. Now the frequency of the r.f. signal generator was adjusted. As soon as this frequency became identical with the center frequency of the spectrum analyzer (which in turn was tuned to the ring resonant frequency), the intensity of the display trace of the swept amplitude analyzer increased drastically over the whole sweeping range. Under this setting, the frequency of the r.f. signal generator output is the required resonance frequency of the ring.

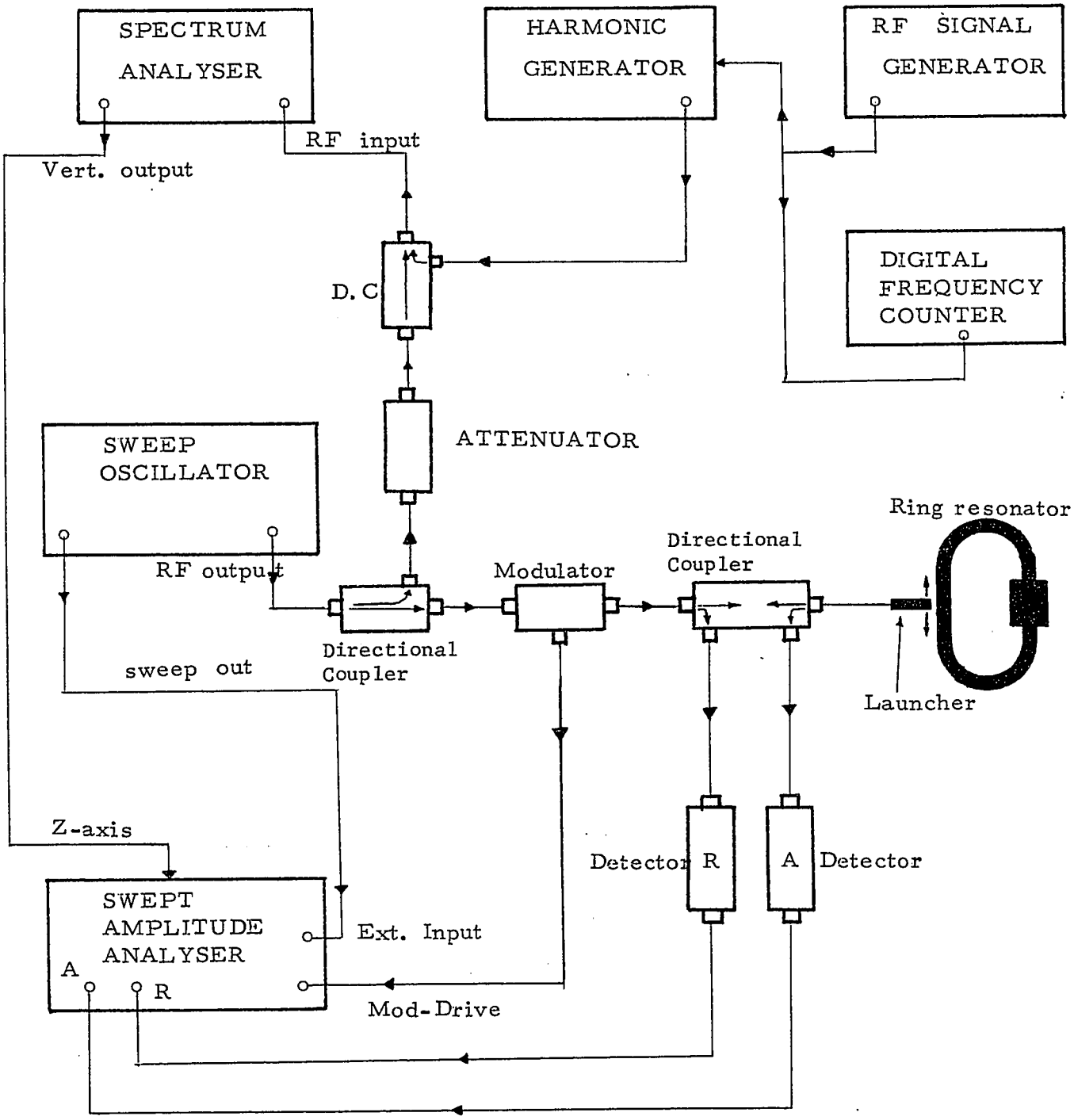

Fig. 3.2: Schematic diagram used for measurement of resonant frequencies.

Both the r.f. signal generator and the frequency counter available for the experiments had a frequency range much smaller than the range (0.1 - 2GHz) over which the ring resonances were being measured. This problem was overcome by inserting a harmonic generator unit between the r.f. signal generator and the spectrum analyzer. By properly choosing the r.f. frequency and using its proper harmonic it was always possible to match any ring resonance frequency.

As mentioned earlier, the accuracy of measurement is limited by the sharpness of the response of the ring. The human error in locating exactly the peak of the ring response cannot be eliminated completely. In order to minimize these errors each resonance frequency was measured five times; the average gave the desired resonance frequency while standard deviation informed about the uncertainty in the measurement.

In the measurement of all resonance frequencies the uncertainty was typically ±16 kHz or less.

3.3 MEASUREMENT OF NOMINAL DIELECTRIC CONSTANT OF THE SUBSTRATE

After measuring the capacitance of the square in the center of the ring, the nominal dielectric constant of the substrate is calculated using the formula:

$$\varepsilon_r = \frac{1}{\varepsilon_o} \frac{C' d}{A}$$

where ε_r = Nominal dielectric constant of the ring.

ε_o = 8.854×10^{-12} farads/meter, permittivity of the free space.

C' = Capacitance of the square in farads.

d = 0.005 meter; spacing between the parallel plates of the capacitor.

A = 16×10^{-4} m^2, the area of the square.

In figure 3.4, the schematic diagram is shown describing the measurement of the capacitance.

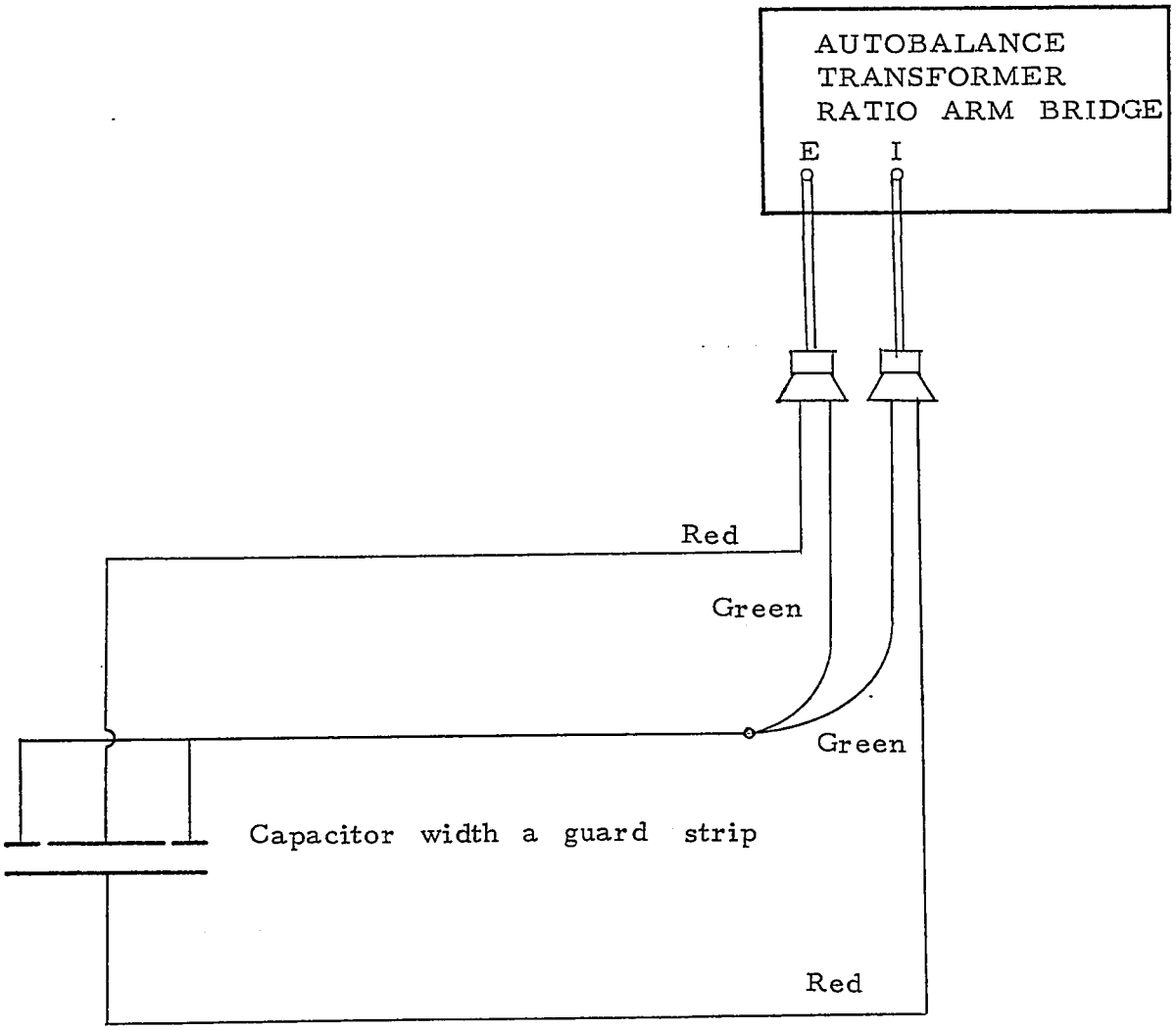

Fig. 3.3: Schematic diagram used for measurement of capacitance.

The transformer ratio bridge measured the capacitance within 0.01% error. Care was taken to balance out the stray capacitances of the leads. To eliminate the errors due to the fringing effect a guard ring was provided. By keeping the square and guard ring at the same potential fringing was practically suppressed.

The nominal dielectric constant of the substrate was $\varepsilon_r = 10.97$.

CHAPTER 4

EXPERIMENTAL RESULTS

The measured resonance frequencies and the detailed analysis necessary for evaluating the step impedance are given in section 4.1. Section 4.2 deals with the error analysis. The experimental results are shown in section 4.3

4.1 COMPUTATIONAL DETAILS

The measured resonance frequencies of the unloaded ring are given in table 1. The resonance frequencies measured; for different line step sizes; for even and odd mode excitation; are given in tables 2 to 6. The computed standard deviation shows the uncertainty in the measurement.

The measured resonance frequencies of the empty ring determine the dispersive characteristics of the ring resonator. To have resonance the length of the ring must equal an integer number of wavelengths.

$$l_{ring} = n\,\lambda_g \tag{4.1}$$

Equation (4.1) can be rewritten as

$$l_{ring} = \frac{n\,c}{\sqrt{\varepsilon_{eff}(f)}\,f_r}$$

solving for the effective dielectric constant:

$$\varepsilon_{eff}(f) = \left[\frac{n\,c}{l_{ring}\,f_r}\right]^2 \tag{4.2}$$

For the different resonant frequencies ε_{eff} is listed in Table 1.

Static characteristic impedance of narrow and wide microstrips have been evaluated using the expression given by Andrew H. Kwon [12], which is given here, for convenience;

$$Z_o = \frac{188.5}{\sqrt{\varepsilon_r}} \left[\frac{w/h}{2} + \frac{\ln 4}{\pi} + \frac{(\varepsilon_r - 1)\ln\left(\frac{e\ \pi^2}{16}\right)}{2\pi\varepsilon_r^2} + \frac{\varepsilon_r + 1}{2\pi\varepsilon_r} \ln\left(\frac{e\pi\left(\frac{w/h}{2} + 0.94\right)}{}\right)\right]^{-1} \quad (4.3)$$

The dynamic characteristic impedance was evaluated as:

$$Z_o(f) = \frac{Z_{o\ air}}{\sqrt{\varepsilon_{eff}(f)}} \quad (4.4)$$

where ε_{eff} for narrow microstrip was computed from (4.2). For wide microstrip $\varepsilon_{eff}(f)$ has been evaluated from the expression given by Jain [13], which is given as:

$$\varepsilon_{eff}(f) = 3x10^{-6}(\varepsilon_r^2 - 1)\ h\ \left[\frac{Z_o}{3}\left(\frac{w'}{h}\right)^2\right]^{\frac{1}{2}}\ (f - f_o) + \varepsilon_{eff_o} \quad (4.5)$$

where

$$f_o = \frac{6.0}{(\varepsilon_r - 1)^{\frac{1}{4}}}\left[\frac{Z_o}{h}\right]^{\frac{1}{2}}$$

and

$$w' = w + \frac{t}{\pi}\left(1 + \ln\frac{2h}{t}\right)$$

ε_r = static relative dielectric constant

ε_{ffo} = static effective dielectric constant

w = width of microstrip in mils

w' = effective width of microstrip

h = separation between microstrip and the ground plane, in mils

t = thickness of microstrip in mils

f_o = frequency in Ghz

f = frequency of interest at which ε_{eff} is to be found, in Ghz

Then, the theoretical value of $\varepsilon_{eff}(f)$ for wide microstrip is obtained by interpolation:

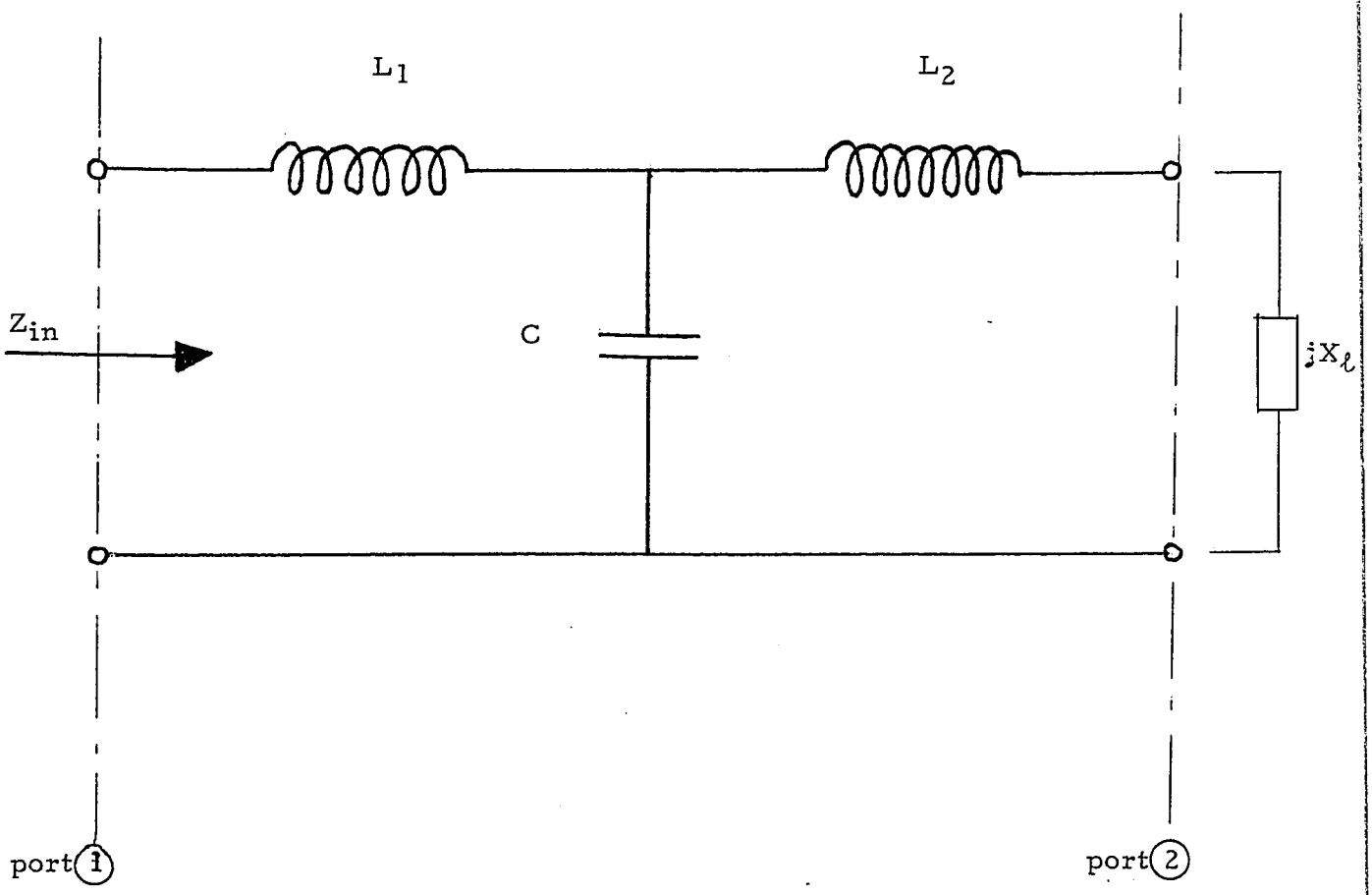

Fig. 4.1: Equivalent representation of the sudden step change in the width of a microstrip.

$$\varepsilon_{eff_w}(f) = \frac{\varepsilon_{eff_w}(f)\ \text{Calculated}}{\varepsilon_{eff_n}(f)\ \text{Calculated}} \times \varepsilon_{eff_n}(f)\ \text{measured} \qquad (4.6)$$

The subscripts w and n stand for wide and narrow microstrips respectively.

The dynamic characteristic impedances and dielectric constants are used to evaluate the step impedance values from (2.19) and (2.20) at various measured frequencies. A computer program has been developed for this purpose and is given in the Appendix A. Measured resonance frequencies and the dimensions of the microstrip are required as data for this program.

The equivalent circuit of the discontinuity can be represented by a T-network as shown in figure 4.1.

The relation between the input impedance; looking into plane 1; in terms of L_1, L_2 and C; when port 2 is terminated by a reactive line impedance j x_e is determined as follows:

$$Z_{in} = j\,x_i = j\omega L_1 + \frac{1}{\frac{1}{1/j\omega C} + \frac{1}{j(\omega L_2 + x_e)}}$$

$$j\,x_i = \frac{j\,[\omega L_1 + \omega L_2 + x_e - \omega^3 L_1 L_2 C - \omega^2 x_e L_1 C]}{1 - \omega^2 L_2 C - \omega x_e C}$$

$$x_i - x_e = \omega(L_1 + L_2) + \omega x_i x_e C + \omega^2 x_i L_2 C - \omega^3 L_1 L_2 C - \omega^2 x_e L_1 C \qquad (4.7)$$

Equation (4.7) forms the basis for solving for L_1, L_2 and C, since the values of x_i and x_e are known from measurements taken at several frequencies.

4.2 ERROR ANALYSIS

A. Chattopadhyay and W. Hoefer [10], have performed an error analysis for the characterization of microstrip discontinuities in resonant rings. The same method is used here.

The expressions for relative error in even and odd mode input admittances are exactly the same, therefore, only the even mode case is considered.

The normalized input admittance is given (from 2.11) as:

$$Y_{ie} = -j \tan \left[\frac{\pi f_{re} \sqrt{\varepsilon_{eff(f)}} \{l_{ring} - l_w\}}{c}\right] \qquad (4.8)$$

since the error in the measurement of Y_{ie} depends on the error with which both unloaded and loaded ring resonance frequencies are determined; therefore,

$$dY_{ie} = \frac{\partial Y_{ie}}{\partial f_r} df_r + \frac{\partial Y_{ie}}{\partial f_{re}} df_{re} \qquad (4.9)$$

where f_r denotes the resonance frequency of the unloaded ring.

Y_{ie} is dependent on the empty resonance frequency implicitly through ε_{eff}. Hence,

$$\frac{\partial Y_{ie}}{\partial f_r} = \frac{\partial Y_{ie}}{\partial\left(\sqrt{\varepsilon_{eff}}\right)} \frac{\partial\left(\sqrt{\varepsilon_{eff}}\right)}{\partial f_r} \qquad (4.10)$$

Using the equation (4.8) and the fact that $\sqrt{\varepsilon_{eff}} = nc/(l_{ring} \cdot f_r)$ when n is an integer, we get,

$$\frac{\partial Y_{ie}}{\partial f_r} = j(1 + |Y_{ie}|^2)\pi (l_{ring} - l_W) \sqrt{\varepsilon_{eff}(f)} \frac{f_{re}}{f_r} \qquad (4.11)$$

Now the dependence of Y_{ie} on f_{re} will be examined. In (4.6) f_{re} appears both explicitly and implicitly (due to the presence of ε_{eff}). It has been found by experiment that ε_{eff} increases linearly with frequency. We can write,

$$\varepsilon_{eff}(f_{re}) = \varepsilon_1 + b\, f_{re}$$

where ε_1 is the effective dielectric constant at zero frequency.

and $b = \partial\varepsilon_{eff}/\partial f$; the slope of the ε_{eff} vs frequency. Using this relation we obtain,

$$\frac{\partial Y_{ie}}{\partial f_{re}} = -j(1 + |Y_{ie}|^2) \frac{\pi l_{ring}}{c} \left[\frac{3\varepsilon_{eff} - \varepsilon_1}{2\sqrt{\varepsilon_{eff}}}\right] \tag{4.12}$$

Combining (4.8), (4.11) and (4.10) we get:

$$dY_{ie} = j(1 + |Y_{ie}|^2) \frac{\pi(l_{ring} - lw)}{c}\left[\sqrt{\varepsilon_{eff}}\frac{f_{re}}{f_r}df_r + \frac{\varepsilon_1 - 3\varepsilon_{eff}}{2\sqrt{\varepsilon_{eff}}} df_{re}\right] \tag{4.13}$$

Under the conditions that

(a) the even and odd resonance frenquencies are very close to each of the unloaded resonance frequencies.

(b) $bf/\varepsilon_1 << 1$.

the expression (4.13) for the relative error in the measurement of input admittance simplifies to:

$$\frac{dY_{ie}}{Y_{ie}} = j\frac{(1 + |Y_{ie}|^2)}{Y_{ie}} \pi\frac{(l_{ring} - lw)}{c}\sqrt{\varepsilon_{eff}}[d_{f_r} - d_{f_{re}}] \tag{4.14}$$

Now the expression for relative error in the measurement of the normalized admittance of the wide microstrip will be obtained similarly. The expression for Y_w from (2.17) is:

$$Y_w = j \tan[\pi\, lw\, f_{re}\sqrt{\varepsilon_{eff_w}(f)}] \tag{4.15}$$

Then;

$$\frac{dY_w}{Y_w} = -j\frac{(1 + |Y_w|^2)}{Y_w} \pi\, l_w\sqrt{\varepsilon_{eff_w}}[d_{f_r} - d_{f_{re}}] \tag{4.16}$$

The relative error in the step admittance is given by:

$$\frac{dY_{step}}{Y_{step}} = \frac{d[Y_{ie} - Y_w]}{Y_{step}} = \frac{dY_{ie} - dY_w}{Y_{step}} \tag{4.17}$$

combining (4.17, (4.16) and (4.14):

$$\frac{dY_{step}}{Y_{step}} = j\pi\left[\frac{d_{f_r} - d_{f_{re}}}{Y_{step}}\right]\left[(1 + |Y_{ie}|^2)\,(l_{ring} - l_w)\sqrt{\varepsilon_{eff}(f)}\,\cdot\right.$$

$$\left. + (1 + |Y_w|^2)\, l_w \sqrt{\varepsilon_{eff_w}(f)}\right] \qquad (4.18)$$

The expression for relative error in the normalized step admittance is given by (4.18). The error analysis was done for every measured value of Y_{ie}, Y_w and Y_{step}.

TABLE: I

Ring without discontinuity

Microstrip width W=0.5315 inch

Temperature inside the chamber=35 Celsius

Frequency [MHz]	Uncertainty in Measurement[KHz]	Guided Wave-length[meters]	Harmonic number	ε_r effective
183.1468	1.328	0.59152	1	7.882
361.1968	3.655	0.29576	2	7.875
539.0790	1.789	0.19718	3	7.955
714.6520	5.367	0.14788	4	8.047
887.4948	4.665	0.11831	5	8.152
1059.0604	8.891	0.09859	6	8.244
1227.8484	5.817	0.08450	7	8.348
1394.6742	7.960	0.07394	8	8.451
1560.2634	4.409	0.06573	9	8.546
1724.7816	10.307	0.05915	10	8.634
1887.4288	11.9733	0.05377	11	8.725

TABLE:II

Step size W_o = 1.579 inch

Even mode excitation

Temperature inside the chamber = 35 Celsius

Frequency [MHz]	Uncertainty in Measurement [KHz]
166.7213	1.735
336.0850	4.100
510.6258	5.980
687.0950	9.890
863.9966	4.820
1038.6556	5.276
1212.9669	6.715
1384.1688	9.600
1553.5167	8.319
1720.4516	13.200
1883.7384	10.763

TABLE:III

Step size Wo=1.579 inch

Odd mode excitation

Temperature inside the chamber=35 Celsius

Frequency [MHz]	Uncertainty in Measurement [KHz]
170.2224	1.857
371.0526	7.242
551.8610	3.256
727.8974	4.821
896.4316	5.200
1058.3962	5.095
1212.5568	7.145
1366.1934	3.747
1522.8708	13.140
1684.5844	15.435
1844.8048	13.717

TABLE IV

Step size W_o=1.227 inch

Even mode excitation

Temperature inside the chamber =35 Celsius

Frequency [MHz]	Uncertainty in Measurement[KHz]
171.7736	3.137
343.4534	2.154
518.0400	4.147
693.7768	2.040
869.9324	5.571
1043.9538	7.250
1217.6430	2.683
1388.4696	3.499
1557.6144	2.940
1724.3904	4.079
1888.0776	5.426

TABLE:V

Step size Wo=1.227 inch
Odd mode excitation
Temperature inside the chamber=35 Celsius

Frequency [MHz]	Uncertainty in Measurement[KHz]
183.3334	1.744
369.6214	6.053
549.8228	3.124
725.5448	2.040
894.7736	2.332
1059.4484	5.571
1217.7174	5.161
1376.2548	6.735
1535.3460	10.564
1696.7984	7.419
1859.1704	9.330

TABLE:VI

Step size Wo=0.893 inch

Even mode excitation

Temperature inside the chamber=35 Celsius

Frequency [MHz]	Uncertainty in Measurement [KHz]
177.1460	2.608
351.9430	2.967
527.2962	3.709
702.2672	3.250
877.3172	5.307
1050.0372	8.060
1222.3488	10.147
1391.9454	2.940
1559.9442	6.997
1725.9080	11.866
1889.3984	14.221

TABLE:VII

Step size Wo=0.893 inch

Odd mode excitation

Temperature inside the chamber =35 Celsius

Frequency [MHz]	Uncertainty in Measurement [KHz]
183.7220	0.002
367.9652	10.167
546.2826	5.535
721.9188	2.713
892.3988	3.487
1060.2116	1.960
1223.7528	5.231
1386.1002	3.600
1547.7132	4.875
1710.2360	6.693
1872.3096	12.290

4.3 EXPERIMENTAL RESULTS

In this section the results of measurements are presented. The dynamic effective dielectric constant of the ring and, the dynamic characterstic impedance for several w/h ratios are plotted in figures 4.2 and 4.3 respectively. The values are accurate to within ± 1 percent due to the uncertainty in the measurement of resonance frequencies. The normalized input impedances Z_{ie}, Z_{io} are shown in figures 4.4 and 4.5 respectively; the impedance corresponding to the step discontinuity is plotted in figure 4.6. These values are accurate to within ± 2 percent due the uncertainty in the dynamic effective dielectric constant and the measured resonance frequencies.

In figures 4.7 and 4.8 the values of the capacitive and the inductive components respectively, are shown for various w/w_o ratios and are compared with the theoretical results obtained by other authors. These results are also tabulated in Table VIII. Since the thesis objective is to obtain the variation of capacitance and inductance of the equivalent circuit versus w/w_o, therefore, the values of L_1, L_2 and C represent the average of the values obtained at several frequencies and it is found that these values are not frequency dependent as assumed in the analysis. The error in the values of L_1, L_2 and C has increased due to the average of several values ; they are accurate to within ± 3 percent. The agreement with the available theoretical values is good.

Table VIII

Measured capacitive and inductive components ($L_1 = L_2$) of the impedance step for several step ratios are given. The theoretical values obtained by other authors are also given for comparasion. Stycast substrate was used. ($\varepsilon_r = 10.97$, h = 5 mm, w/h = 2.7, and $Z_{01} = 26$ ohms).

w/w_o	Z_{02}	L obtained by measurement	L obtained by Gopinath et al	C obtained by measurement	C obtained by Farrar & Adams
0.337	11	26×10^{-11}	24.8×10^{-11}	0.800×10^{-12}	0.779×10^{-12}
0.433	14	16×10^{-11}	15.0×10^{-11}	0.502×10^{-12}	0.463×10^{-12}
0.595	18	7×10^{-11}	6.7×10^{-11}	0.237×10^{-12}	0.221×10^{-12}

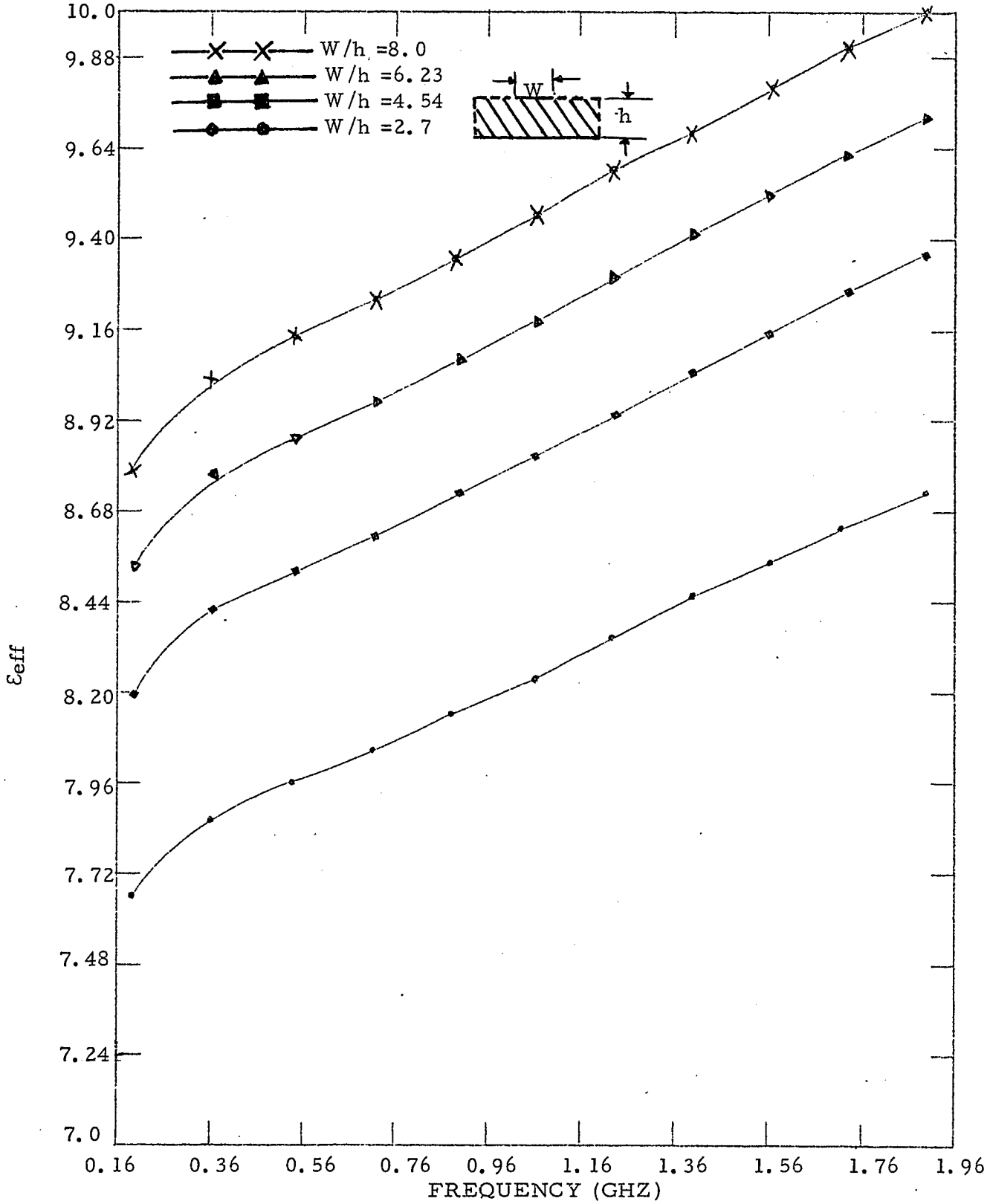

Fig. 4.2: Dynamic effective dielectric constant Vs frequency for microstrips of different widths on Stycast substrate (ε_r=10.97, h=5 mm)

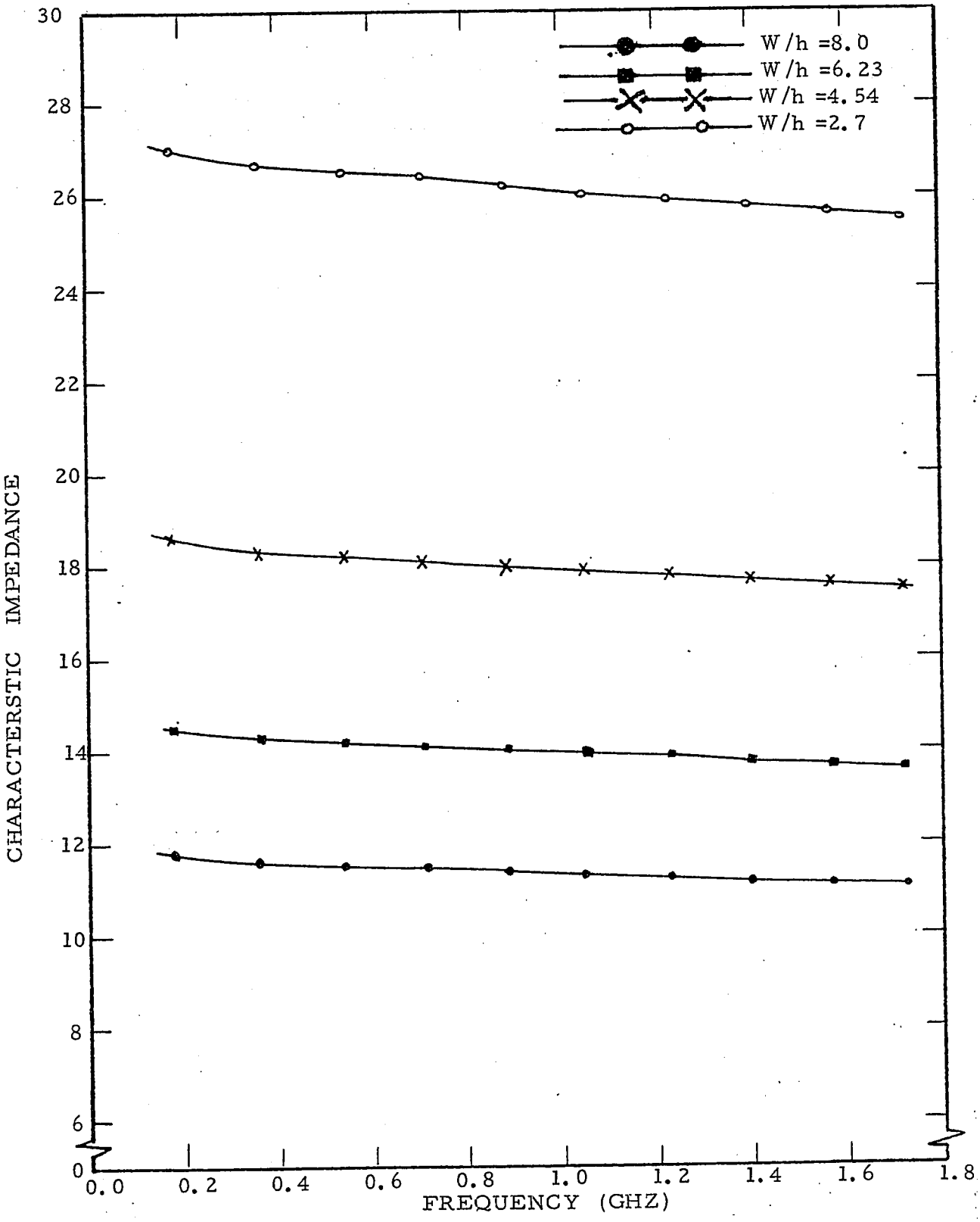

Fig. 4.3: Dynamic characterstic impedance Vs frequency for different W/h ratios. Stycast substrate (ε_r=10.97, h=5 mm)

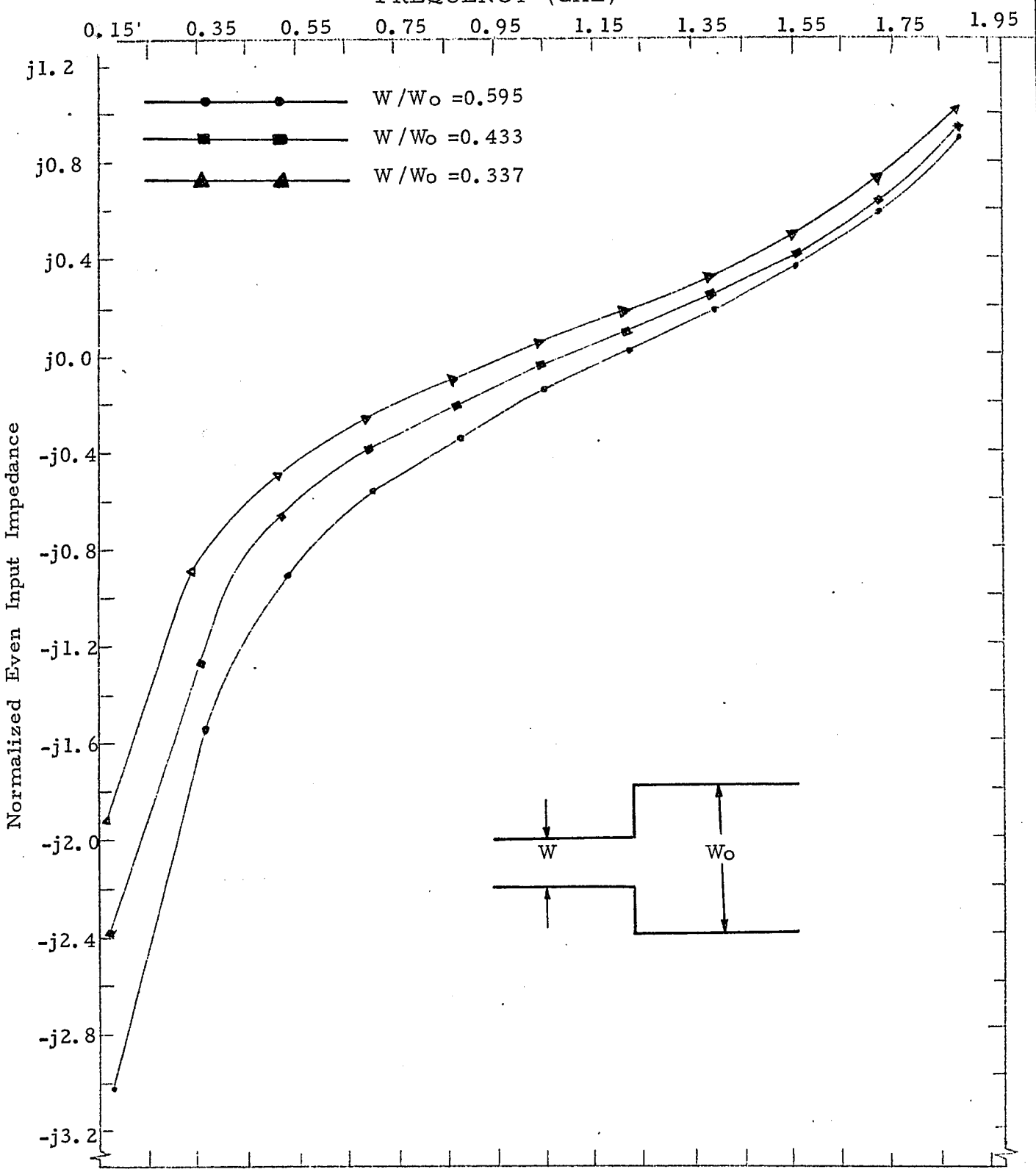

Fig. 4.4: Normalized even input impedance corresponding to the step change in the width of microstrip on the Stycast substrate (ε_r=10.97, h=5 mm and Zo=26 Ohms)

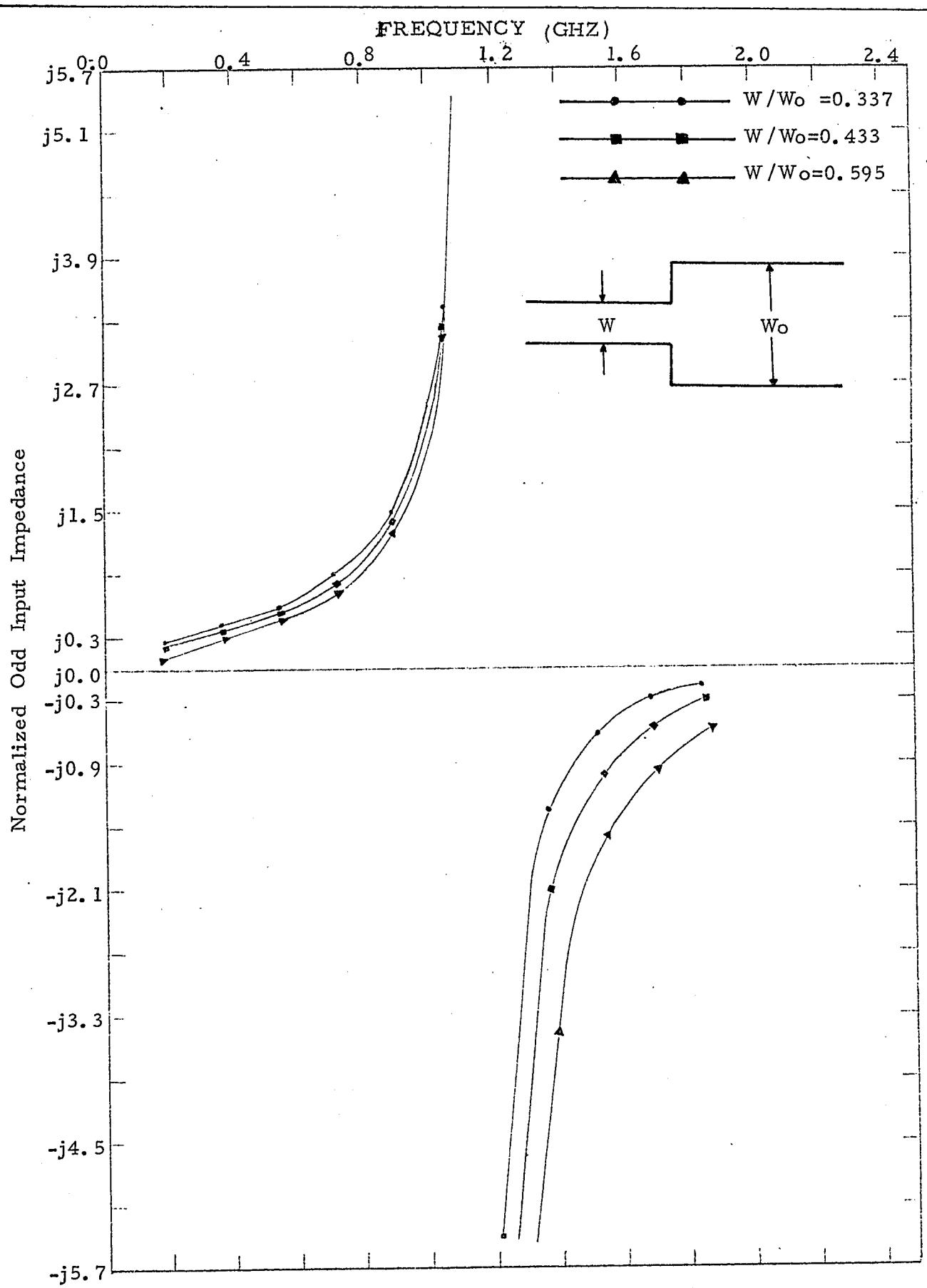

Fig. 4.5: Normalized odd input impedance corresponding to the step change in the width of microstrip line on Stycast substrate (ε_r=10.97, h=5 mm, W/h =2.7 & Zo=26 Ohms)

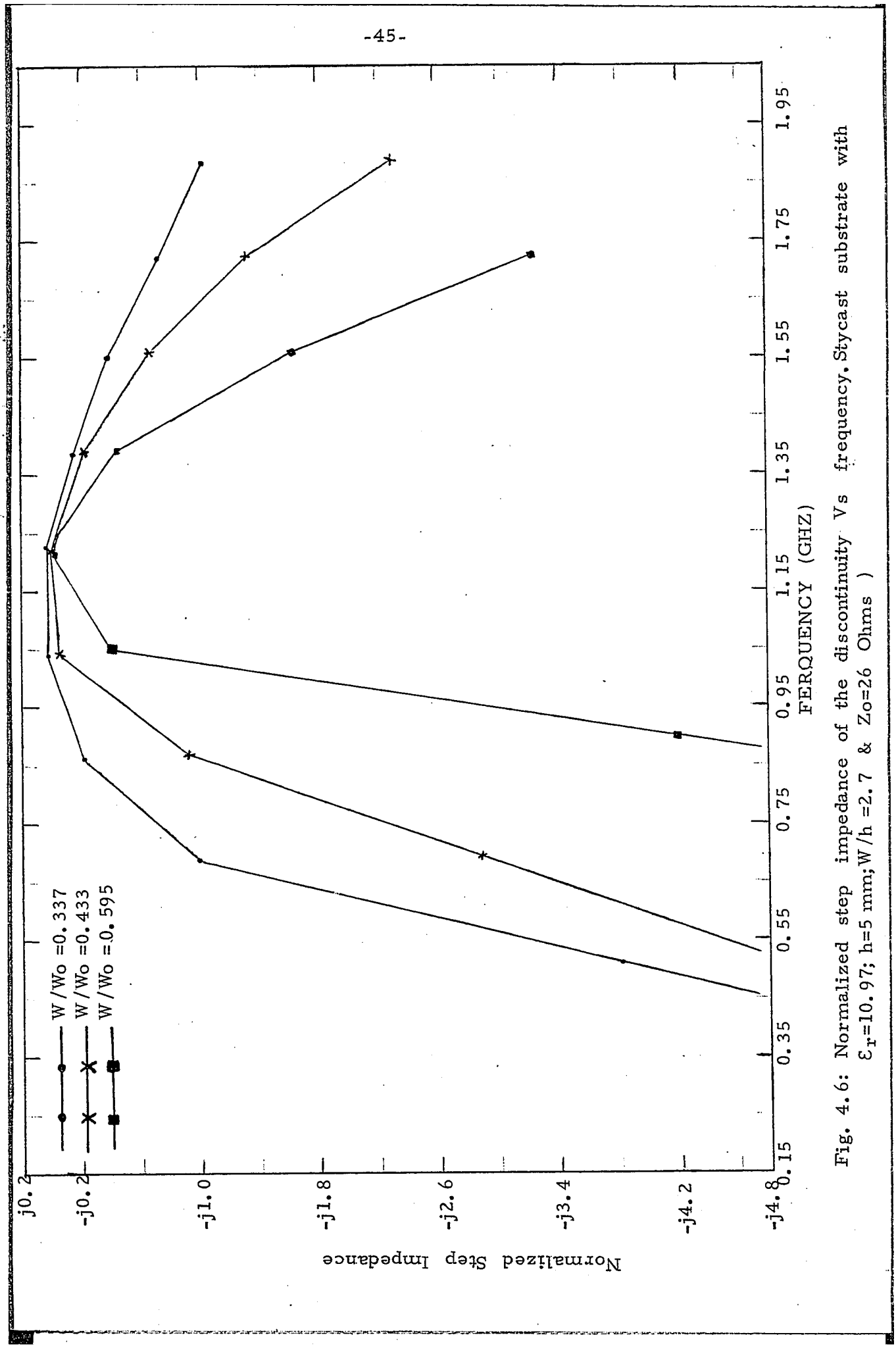

Fig. 4.6: Normalized step impedance of the discontinuity Vs frequency. Stycast substrate with ε_r=10.97; h=5 mm; W/h =2.7 & Zo=26 Ohms)

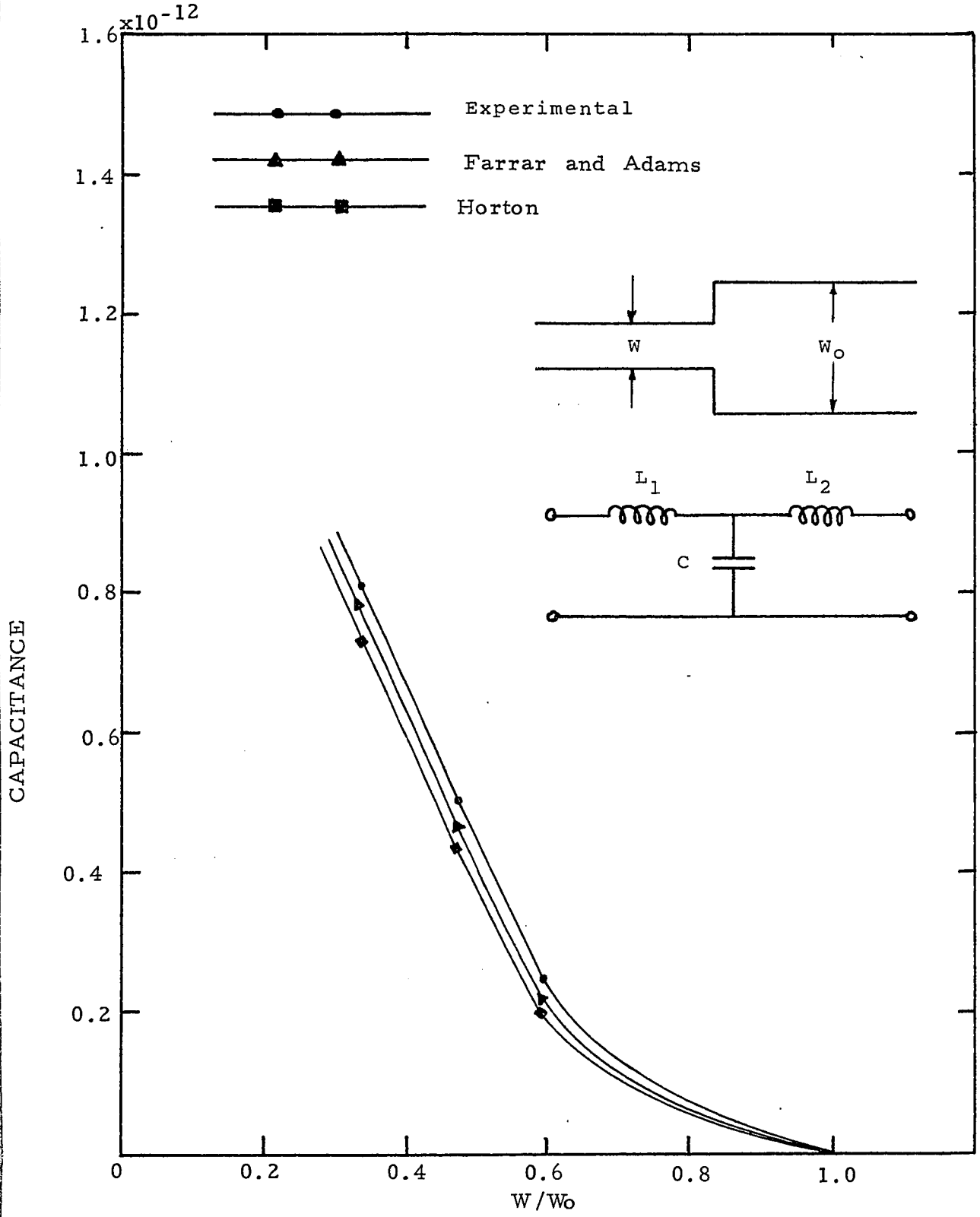

Fig 4.7: Capacitance associated with the step impedance Vs W/Wo. Stycast substrate (εr=10.97, h=5 mm, W/h =2.7 and Zo=26 ohms)

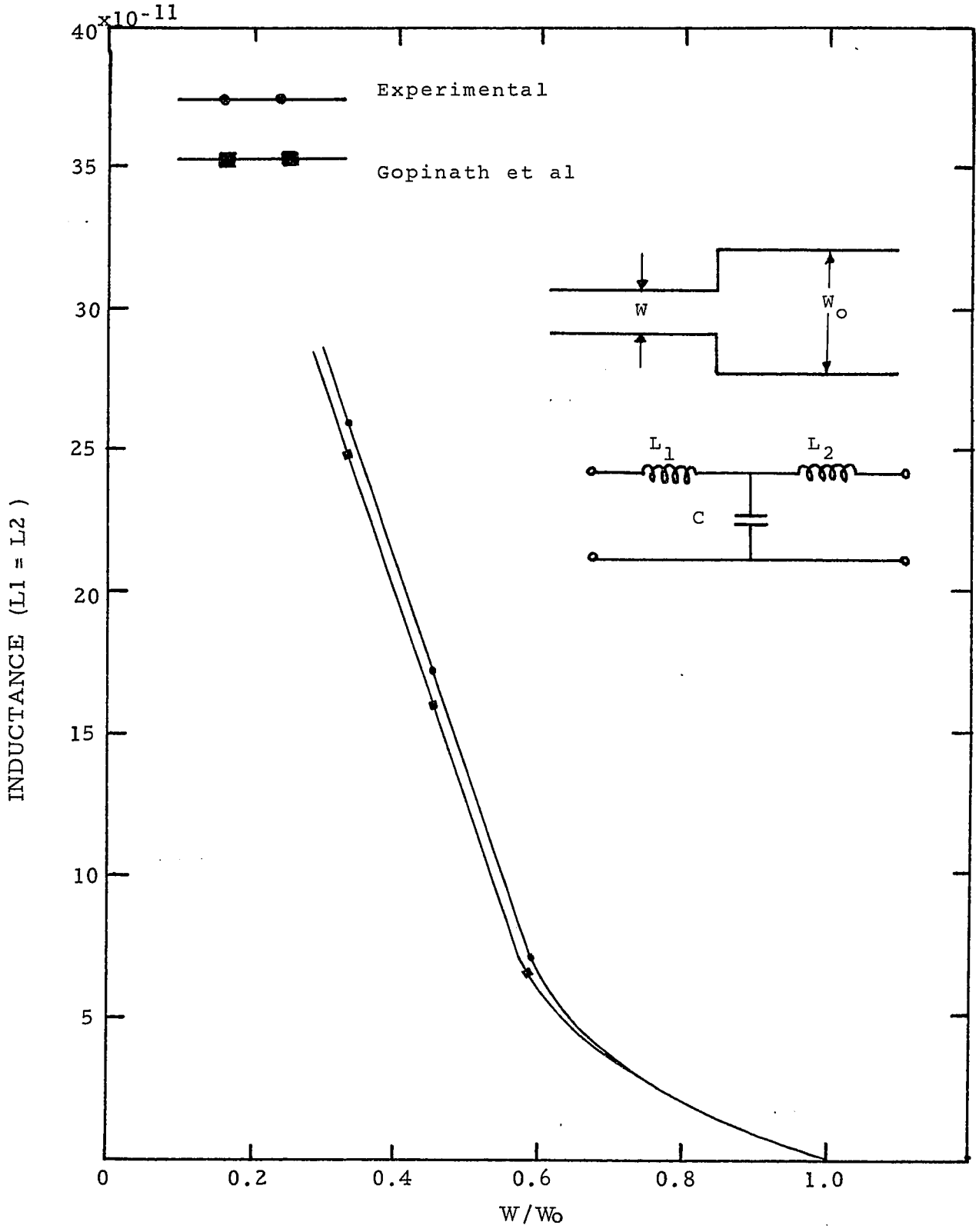

Fig. 4.8; Inductance associated with the step impedance Vs W/Wo.
Stycast substrate (εr=10.97; h=5 mm, W/h =2.7, and Zo=26 ohms)

4.4 CONCLUSION

The resonant ring method has been applied to determine the parameters of the step discontinuity. The values of the capacitive and the inductive elements of the equivalent circuit of the discontinuity are accurate to within ± 3 percent and are independent of frequency of operation. The results agree well with the theoretical values reported by other authors, and thus, confirm very well the existing theories and are a valid contribution to the knowledge of the behaviour of the impedance steps.

APPENDIX A

A computer program, written in Fortran IV, is presented in this appendix. It calculates $\varepsilon_{eff}(f)$ (using the straight line approximation) and $Z_o(f)$ for wide and narrow microstrips; Y_{io}, Y_{io}, Y_{we}, Y_{wo}, and Y_{step} at the several measured resonance frequencies according to expressions given in Chapters 2 and 4. The dimensions of microstrips and measured resonance frequencies are fed in as data. For example, the output for w = 0.5315 inch and w_o = 1.579 inch for even excitation is given.

```
      C     THIS PROGRAM CALCULATES STATIC AND DYNAMIC CHARACTERSTIC
      C     IMPEDANCES,DYNAMIC EPSILEN EFFECTIVE FOR MICROSTRIPS.
      C     EVEN AND ODD INPUT ADMITTANCES,WIDE MICROSTRIP LINE ADMITTANCE
      C     STEP ADMITTANCES AND ERROR ANALYSIS FOR  Y-STEP,Y-IN & Y-WIDE LINE
      C     ARE ALSO EVALUATED BY THIS PROGRAM.
0001        REAL*8 H,W,D1,C1,F1,F2,F3,ZP,Z0,F,W1,F0,C2,C3,C4,EFF2,WK
0002        REAL*8 FRE(11)
0003        REAL*8 EFFS,EFF ,T
0004        REAL*8 DLOG
0005        REAL*8    X(2),Y(2)
0006        REAL* 8 DABS
0007        REAL*8    EFS(11),EFS1(22),ZK(11)
0008        REAL*8    ZK1(11),EFFW(11)
0009        REAL*8 XN,XYZ,YUU1(11),ZUU1(11),YUU(11),ZUU(11)
0010        REAL*8    FR(11)
0011        REAL*8    XF,C,RI,X1,X2,SLOPE,SLOP1,SLOP2,SLOP,Z01,Z02
0012        REAL*8 DSQRT
0013        REAL*8 EF01,EF02,EF1,EF2,DCOTAN,DTAN,Z,YT,ZL,YL,A,ZU,YU,ZU1,YU1
0014        REAL*8 PI
0015        REAL*8 WC,WM,WW
0016        E=2.718281
0017        PI=3.141593
0018        RI=.5915252-0.04
0019        C=299.7925
0020        L=1
0021        H10=0.5
0022        H=H10*1000./2.54
0023        READ(5,61) (EFS(I),I=1,11)
0024        READ(5,62) (FR(I),I=1,11)
0025        DO 3 I=1,2
0026        READ(5,62) W10
0027        W=W10*1000.
0028        DO 2 J=1,2
0029        EPS=10.97
0030        IF(J.EQ.1)  EPS=1.
0031      1 D1=188.5/SQRT(EPS)
0032        C1=(EPS+1.)/(2.*PI*EPS)
0033        F1=W/(H*2.)+DLOG(4.D0)/PI
0034        XYZ=E*PI*PI/16.
0035        F2=(EPS-1.)*DLOG(XYZ)/(2.*PI*EPS*EPS)
0036        XN=(PI*E*(W/(H*2.)+0.94))/2.
0037        F3=DLOG(XN)
0038        ZP=D1/(F1+F2+C1*F3)
0039        Z0=ZP
0040        Y(J)=ZP
0041      2 CONTINUE
0042        EFFS=(Y(1)/Y(2))**2
0043        EFF=EFFS
0044        X(I)=EFFS
0045        PRINT 101
0046        PRINT 109
0047        IF(I-1) 34,34,35
0048     34 PRINT 105
0049     35 KISHO=1
0050        IF(I-1)36,36,37
0051     37 PRINT 107
0052      36 PRINT 103,Y(1),Y(2)
0053        PRINT 102,EFFS
```

```
0054                DO 15 J=1,11
0055                IF(I.EQ.1) ZK(J)=Y(1)/DSQRT(EFS(J))
0056                F=FR(J)/1000.
0057                T=5.
0058                W1=W+(T/PI)*(1.+DLOG(2.D0*H/T))
0059                F0=DSQRT(Z0/H)*6./(EPS-1.)**0.25
0060                C2=3.D-6
0061                C3=(EPS*EPS-1.)*H*(F-F0)
0062                C4=DSQRT(Z0*W1/H)
0063                EFF2=C2*C3*C4+EFF
0064                EFS1(L)=EFF2
0065                IF(I-1) 30,30,31
0066          30    PRINT 100,EFF2,FR(J),ZK(J)
0067                PRINT 110,J
0068          31     KAMAL =1
0069                IF(I-1) 32,32,33
0070          33    PRINT 106,EFF2,FR(J)
0071          32    L=L+1
0072          15    CONTINUE
0073          3     CONTINUE
0074                PRINT 101
0075                DO 8 I=1,11
0076                EFFW(I)=EFS(I)*EFS1(I+11)/EFS1(I)
0077                ZK1(I)=Y(1)/DSQRT(EFFW(I))
0078                PRINT 104,EFFW(I),ZK1(I)
0079                PRINT 108,I
0080          8      CONTINUE
0081                PRINT 101
0082                PRINT 109
0083                PRINT 107
0084                PRINT 121
0085                PRINT 120
0086                PRINT 128
0087                READ(5,63) (FRE(I),I=1,11)
0088                DO 5 J=1,11
0089                I=1
0090                XF=FRE(J)
0091          6     IF(XF.LT.FR(I)) GO TO 4
0092                I=I+1
0093                IF(I.LE.11) GO TO 6
0094                I=I-1
0095          4     BIG=FR(I)
0096                IF(I.EQ.1)  I=2
0097                X1=FR(I)-FR(I-1)
0098                X2=FRE(J)-FR(I)
0099                SLOPE=(EFS(I)-EFS(I-1))
0100                EF01=SLOPE*X2/X1+EFS(I)
0101                SLOP1=(ZK(I)-ZK(I-1))
0102                Z01=SLOP1*X2/X1+ZK(I)
0103                SLOP2=(ZK1(I)-ZK1(I-1))
0104                Z02=SLOP2*X2/X1+ZK1(I)
0105                SLOP=(EFFW(I)-EFFW(I-1))
0106                EF02=SLOP*X2/X1+EFFW(I)
0107                EF1=(EF01)**0.5
0108                EF2=(EF02)**0.5
0109                Z=DCOTAN((PI*RI*FRE(J)*EF1)/C)
0110                YT=-1./(Z*Z01)
0111                ZL=-DCOTAN((0.04*PI*FRE(J)*EF2)/C)
```

```
0112                YL=-1./(ZL*Z02)
0113                A=YT-YL
0114                YU=A
0115                ZU=-1./YU
0116                ZU1=ZU/Z01
0117                YU1=-1./ZU1
0118                WK=(PI*6./C)*(EF1*RI*(1.+DABS(Z )*DABS(Z ))+
                   1EF2*0.04*(1.+DABS(ZL)*DABS(ZL)))
0119                WK=WK*DABS(A)*Z01
0120                 WC=((PI*EF1*6.*RI/C)*(1.+DABS(Z )*DABS(Z )))/DABS(Z )
0121                WW=((PI*EF2*6.*0.04/C)*(1.+DABS(ZL)*DABS(ZL)))/DABS(ZL)
0122                PRINT 119,WK,WC,WW,YU1,Z ,ZL,FRE(J)
0123          5     CONTINUE
0124                PRINT 101
0125         119    FORMAT('-',F13.6,1X,F11.6,2X,F11.6,3X,F11.6,3X,F11.6,4X,F11.6,5)
                   1F11.6)
0126         128    FORMAT('-',1X,'P ERROR IN ZS',2X,'PE ZIN   ',3X,' PE IN ZL  ',3)
                   1,'YU NORMALZD',3X,'Z IN NORMZ',3X,'Z LINE NORMLZ',3X,'FREQ MHZ'
0127         120     FORMAT('-')
0128         121    FORMAT('-',50X,'EVEN MODE RES FREQUENCIES')
0129         101     FORMAT('1')
0130         103    FORMAT('-',10X,'Z0 AIR =',F11.6,10X,'Z0 STATIC =',F11.6)
0131         102    FORMAT('-','EFF STATIC =',F11.6)
0132         100    FORMAT('-',10X,'EPS DYNAMIC =',F11.6,10X,'FREQ MHZ =',F9.4,
                   110X,'Z0(  )=',F11.6)
0133         108    FORMAT('+',47X,I2)
0134         110     FORMAT('+',76X,I2)
0135         106    FORMAT('-',10X,'EPS DYNAMIC =',F11.6,10X,'FREQ MHZ =',F9.4)
0136         104    FORMAT('-',10X,'EFF DYNAMIC =',F11.6,10X,'Z0(  )=',F11.6)
0137         109    FORMAT('-',50X,'BOX NOT COVERED')
0138         105    FORMAT('-',50X,'STRIP WIDTH = 0.5315 INCHES')
0139         107     FORMAT('-',50X,'STRIP WIDTH = 1.579 INCHES')
0140         61     FORMAT(5D14.10)
0141         62     FORMAT(F14.7)
0142         63     FORMAT(8F10.4)
0143                STOP
0144                END
```

BOX NOT COVERED

STRIP WIDTH = 0.5315 INCHES

Z0 AIR = 74.888628 Z0 STATIC = 25.939238

STATIC = 8.335225

EPS DYNAMIC =	7.715394	FREQ MHZ = 183.1468	Z0(1)= 27.
EPS DYNAMIC =	7.821249	FREQ MHZ = 361.1968	Z0(2)= 26.
EPS DYNAMIC =	7.927005	FREQ MHZ = 539.0790	Z0(3)= 26.
EPS DYNAMIC =	8.031387	FREQ MHZ = 714.6520	Z0(4)= 26.
EPS DYNAMIC =	8.134147	FREQ MHZ = 887.4948	Z0(5)= 26.
EPS DYNAMIC =	8.236147	FREQ MHZ =1059.0604	Z0(6)= 26.
EPS DYNAMIC =	8.336496	FREQ MHZ =1227.8484	Z0(7)= 25
EPS DYNAMIC =	8.435678	FREQ MHZ =1394.6742	Z0(8)= 25
EPS DYNAMIC =	8.534125	FREQ MHZ =1560.2634	Z0(9)= 25
EPS DYNAMIC =	8.631935	FREQ MHZ =1724.7816	Z0(10)= 25
EPS DYNAMIC =	8.728633	FREQ MHZ =1887.4288	Z0(11)= 25

BOX NOT COVERED

STRIP WIDTH = 1.579 INCHES

Z0 AIR = 34.758549 Z0 STATIC = 11.408500

STATIC = 9.282526

EPS DYNAMIC = 8.856821	FREQ MHZ = 183.1468
EPS DYNAMIC = 8.977186	FREQ MHZ = 361.1968
EPS DYNAMIC = 9.097436	FREQ MHZ = 539.0790
EPS DYNAMIC = 9.216126	FREQ MHZ = 714.6520
EPS DYNAMIC = 9.332970	FREQ MHZ = 887.4948
EPS DYNAMIC = 9.448951	FREQ MHZ =1059.0604
EPS DYNAMIC = 9.563054	FREQ MHZ =1227.8484
EPS DYNAMIC = 9.675830	FREQ MHZ =1394.6742
EPS DYNAMIC = 9.787771	FREQ MHZ =1560.2634
EPS DYNAMIC = 9.898987	FREQ MHZ =1724.7816
EPS DYNAMIC = 10.008939	FREQ MHZ =1887.4288

EFF DYNAMIC =	8.790553	Z0(1)=	11.723399
EFF DYNAMIC =	9.039244	Z0(2)=	11.561005
EFF DYNAMIC =	9.129424	Z0(3)=	11.503763
EFF DYNAMIC =	9.233884	Z0(4)=	11.438510
EFF DYNAMIC =	9.354316	Z0(5)=	11.364638
EFF DYNAMIC =	9.458371	Z0(6)=	11.301952
EFF DYNAMIC =	9.576691	Z0(7)=	11.231918
EFF DYNAMIC =	9.693899	Z0(8)=	11.163809
EFF DYNAMIC =	9.801889	Z0(9)=	11.102141
EFF DYNAMIC =	9.901710	Z0(10)=	11.046038
EFF DYNAMIC =	10.004188	Z0(11)=	10.989318

BOX NOT COVERED

STRIP WIDTH = 1.579 INCHES

EVEN MODE RES FREQUENCIES

P ERROR IN ZS	PE ZIN	PE IN ZL	YU NORMALZD	Z IN NORMZ	Z LINE NORMLZ
0.021525	0.234422	0.037036	0.034264	-1.927222	-4.763407
0.018310	0.195538	0.020171	0.083561	-0.891314	-2.222975
0.037515	0.244551	0.015794	0.262302	-0.499205	-1.325850
0.119553	0.396778	0.015517	1.011767	-0.265106	-0.836140
0.503779	0.921130	0.019200	4.592081	-0.108665	-0.500571
3.053334	1.850745	0.034446	-28.283025	0.053920	-0.237005
144.136310	0.581209	4.392955	1297.560670	0.177739	0.001771
0.785265	0.342907	0.034571	6.561005	0.324901	0.239394
0.348508	0.254371	0.019569	2.557939	0.496783	0.504797
0.234419	0.213879	0.016070	1.380858	0.730684	0.839174
0.204630	0.205754	0.016562	0.824190	1.099562	1.330810

REFERENCES

[1] I. Wolff, G. Kompa, and R. Mehran: "Calculation method for microstrip discontinuities and T junctions", Electronics letters, Vol. 8 No. 7, 6th April, 1972, pp. 177-179.

[2] A. Farrar, and A.T. Adams: "Matrix methods for microstrip three dimensional problems", I.E.E.E. Trans. on Microwave Theory and Tech., Vol. MTT-20, No. 8, August 1972, pp. 497-504.

[3] R. Horton: "Equivalent representation of an abrupt impedance step in microstrip Line", IEEE Trans. on Microwave Theory and Tech., Vol. MTT-21, No. 8, August 1973, pp. 562-564.

[4] H. Groll, and W. Weidmann: "Measurement of equivalent circuit elements of microstrip discontinuities by a resonant method", NTZ-Aufsatze - microwave measurements, NTZ (1975), H.2, S. 74-77.

[5] S. Akhtarzad, and P.B. Johns: "Three dimensional transmission line matrix computer analysis of microstrip resonators", IEEE Trans. on Microwave Theory and Tech., Vol. MTT-22, No. 12, December 1975, pp. 990-997.

[6] A. Gopinath, A.F. Thomson, and I.M. Stephenson, "Equivalent circuit parameters of microstrip step change in width and cross junctions", IEEE Trans. on Microwave Theory and Tech., Vol. MTT-24, No. 3, March 1976, pp. 142-144.

[7] H.A. Wheeler: "Transmission line properties of parallel strips separated by a dielectric sheet", IEEE Trans. on Microwave Theory and Tech., Vol. MT T-13, March 1965, pp. 172-185.

[8] W.J.R. Hoefer, and A. Chattopadhyay: "Evaluation of the equivalent circuit parameters of microstrip discontinuities through perturbation of a resonant ring", IEEE Trans. on Microwave Theory and Tech., Vol. MTT-23, No. 12, December 1975, pp. 1067-1071.

[9] B. Easter: "Equivalent circuits of some microstrip discontinuities", IEEE Trans. on Microwave Theory and Tech. Vol. MTT-23, August 1975, pp. 665-660.

[10] A. Chattopadhyay and W.J.R. Hoefer: "Error analysis of microstrip discontinuities in resonant rings", IEEE 1975 Conference Digest, held in Toronto, Canada from Sept. 29 to Oct. 1, 1975, pp. 28-29, Paper No. 75041, Session No. 4.

[11] W.J.R. Hoefer and G.R. Painchaud: "Frequency markers providing measurements", Electronics letters Vol. 10, pp. 123-124, April 1974.

[12] A.H. Kwon: "Design of Microstrip transmission line", Microwave Journal, International Edition, Vol. 19, No. 1, pp. 61-63, January 1976.

[13] O.P. Jain: "A study of dispersive behaviour in microstrip transmission lines", Faculty of Engg., Carleton University, Ottawa, Ontario, Canada, Tech. report, pp. 10-19, May 1971.

[14] A. Chattopadhyay and W. Hoefer, "General Analysis of Measurement of microstrip discontinuity parameters in a resonant ring", Technical report no: TR-76-1, pp. 10-17, dept. of Electrical Engineering, University of Ottawa, Ottawa, Canada.